GL02135

Ore Geology Reviews, 7 (1992) 193–223
Elsevier Science Publishers B.V., Amsterdam — Printed in The Netherlands

Contrasting styles of epithermal precious-metal mineralization in the southwestern Nevada volcanic field, USA

Stephen B. Castor[a] and Steven I. Weiss[b]

[a]*Nevada Bureau of Mines and Geology, Mackay School of Mines, University of Nevada, Reno, NV 89557, USA*
[b]*Department of Geological Sciences, Mackay School of Mines, University of Nevada, Reno, NV 89557, USA*

(Received August 27, 1991; accepted after revision January 27, 1992)

ABSTRACT

Castor, S.B. and Weiss, S.I., 1992. Contrasting styles of epithermal precious-metal mineralization in the southwestern Nevada volcanic field, USA. *Ore Geol. Rev.*, 7: 193–223.

The southwestern Nevada volcanic field contains epithermal precious-metal deposits hosted by Miocene volcanic rocks and pre-Tertiary sedimentary rocks with production + reserves greater than 60 t of gold and 150 t of silver. The volcanic rocks consist predominantly of ash-flow tuffs erupted between 15 and 7 Ma during three major magmatic stages: the main stage (ca. 15–13 Ma); the Timber Mountain stage (ca. 13–9 Ma); and the late stage (ca. 9–7 Ma). Hydrothermal activity and precious-metal mineralization in the southern part of the field took place between ca. 13 and 8.5 Ma, coinciding with portions of all three magmatic stages. Regional extension during this period produced imbricate normal and detachment faulting that provided structural control for some of the mineralization.

Contrasts in the style and geochemistry of mineralization, together with stratigraphic and radiometric age data and differences in geologic setting reflect the variable nature of hydrothermal activity during development of the southwestern Nevada volcanic field. During the main magmatic stage, silver-rich vein mineralization of the adularia-sericite type occurred in an intermediate volcanic center at Wahmonie. Secondary high-salinity fluid inclusions in felsic subvolcanic intrusions, a trace element suite that includes bismuth and tellurium, and geophysical data support the presence of a buried porphyry-type magmatic system at Wahmonie.

Hydrothermal activity at Bare Mountain took place during the main magmatic stage, and may have continued into the Timber Mountain magmatic stage. Bare Mountain contains gold-rich, disseminated Carlin-type deposits with high arsenic, antimony, mercury and fluorine in sedimentary and igneous rocks. In northern and eastern Bare Mountain, mineralization is associated with felsic porphyry dikes that contain secondary high-salinity fluid inclusions. A genetic relationship between porphyry magmatism and shallow Carlin-type gold deposits seems likely at Bare Mountain.

Sedimentary-rock-hosted mineralization at Mine Mountain is spatially associated with a thrust fault and was apparently deposited, in part, by a hydrothermal system active during the Timber Mountain magmatic stage. The silver:gold ratio is high and base-metal, arsenic, antimony, mercury and selenium contents are very high. Mine Mountain mineralization shares features with vein and disseminated silver deposits at Candelaria, Nevada.

Gold-silver deposits in the areally extensive Bullfrog district comprise the largest known precious-metal resource in the volcanic field. They are mainly quartz-carbonate ± adularia veins with alteration and mineralization styles similar to other adularia-sericite-type deposits in the Great Basin. Deposits in the Rhyolite area and at the Gold Bar mine have very low contents of arsenic and mercury compared to other epithermal deposits in the Great Basin, although copper and antimony are locally elevated. Similarities in mineralization style and assemblages, which include two occurrences of the rare gold-silver sulfide uytenbogaardtite, indicate deposition under similar conditions in different parts of the district. Hydrothermal activity in the Bullfrog district was coeval with extensional tectonism and may have continued from the Timber Mountain stage into the late magmatic stage. Mineralization at some deposits in the Bullfrog and Bare Mountain districts is spatially associated with, and, in part, structurally controlled by a regional detachment fault system. However, significant differences in age, mineralization style and geochemistry indicate that mineralization in the two districts is unrelated.

Correspondence to: S.B. Castor, Nevada Bureau of Mines and Geology, Mackay School of Mines, University of Nevada, Reno, NV 89557, USA.

Introduction

The southwestern Nevada volcanic field (SWNVF) consists of middle- to late-Miocene volcanic rocks that once covered an area of more than 10,000 km^2 (Byers et al., 1989), centered about 150 km northwest of Las Vegas (Fig. 1). The southern part of the SWNVF contains precious-metal deposits that have been exploited intermittently from the mid 19th century to the present. These deposits are hosted by volcanic rocks of the SWNVF and underlying pre-Tertiary sedimentary rocks.

In the course of more than three decades of geologic investigations, conducted mainly in support of nuclear weapons testing and proposed nuclear-waste storage programs, the SWNVF has become one of the most studied intracontinental volcanic fields in the world. Considerable efforts have been directed toward understanding the intense, long-lived history of magmatic and volcanic activity, caldera geology, volcano-tectonic evolution, and Neogene structural setting of the SWNVF. Investigations of hydrothermal activity and mineralization in the SWNVF have mostly been limited to reports on individual ore deposits and mineralized districts (e.g., Ransome et al., 1910; Cornwall and Kleinhampl, 1964; Tingley, 1984; Jorgensen et al., 1989) or to mineral inventories of large areas that include parts of the SWNVF (e.g., Cornwall, 1972; Quade et al., 1984). Jackson (1988) summarized time–space patterns of hydrothermal activity and mineralization, and proposed that hydrothermal activity and epithermal mineralization in the southern part of the SWNVF were related to magmatic and volcanic activity at major volcanic centers. More recently, Noble et al. (1991) proposed that hydrothermal activity and mineralization were associated with specific magmatic stages in the development of the SWNVF. However, comparisons of geologic and geochemical features of precious-metal deposits for the SWNVF as a whole are lacking.

In this paper we compare geologic settings, geochemical characteristics, mineralization and alteration assemblages, and general styles

Stephen Castor graduated from the University of California, Riverside (1965) and obtained a Ph.D. from the University of Nevada, Reno (1972). He has worked for more than twenty years as an economic geologist, studying deposits of a wide variety of mineral commodities. Current research interests include the geology of rare metal, industrial mineral and gold deposits.

Steven Weiss graduated from The Colorado College (1978) and obtained an M.Sc. degree from the University of Nevada, Reno (1987). He has worked as an economic geologist for 11 years, primarily on mineral deposits in volcanic terranes. Current research includes precious-metals hydrothermal systems associated with silicic volcanic centers, caldera geology and large-volume pyroclastic volcanism, and the interaction of high-level silicic magmatic-volcanic activity with detachment-style extenional faulting.

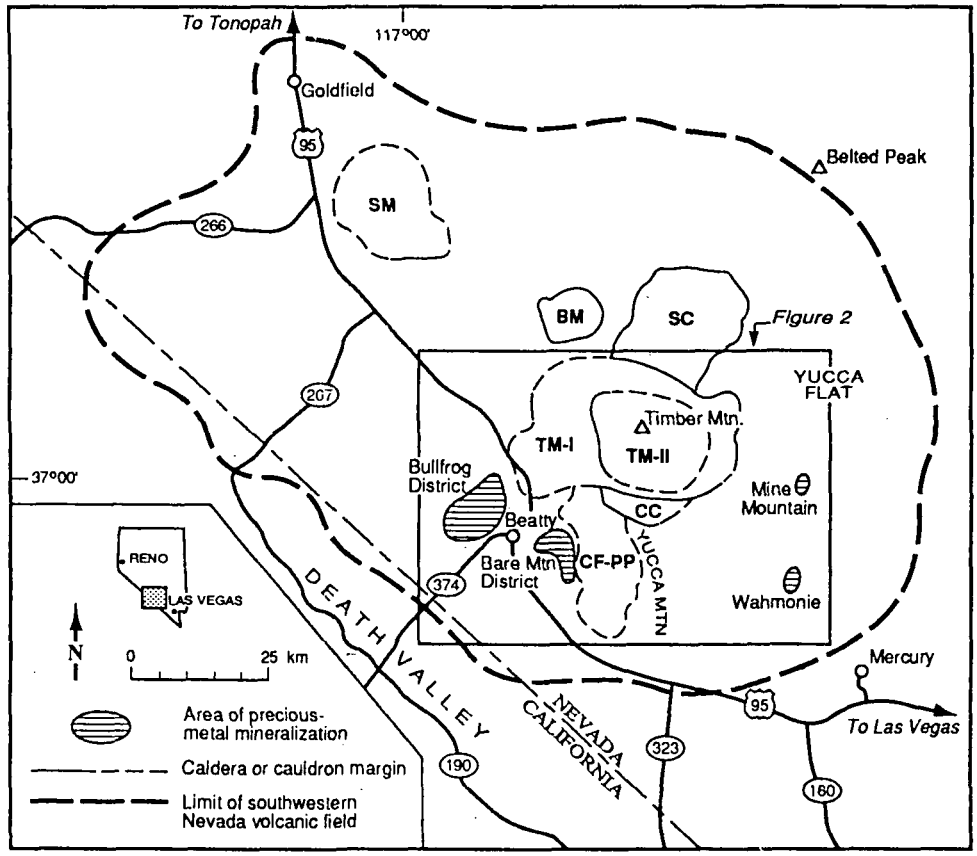

Fig. 1. Map of the southwestern Nevada volcanic field showing major volcanic centers and mineralized areas. (Modified from Noble et al., 1991; and Byers et al., 1989.) *BM*=Black Mountain caldera, *CF–PP*=Inferred Crater Flat–Prospector Pass caldera complex, *CC*=Claim Canyon cauldron, *SC*=Silent Canyon caldera, *SM*=Stonewall Mountain volcanic center, *TM-I*=Timber Mountain caldera complex I, *TM-II*=Timber Mountain caldera complex II. Heavy dashed line is approximate limit of SWNVF.

of mineralization of four selected areas in the southern part of the SWNVF: the Bullfrog district; northern and eastern Bare Mountain; the Wahmonie district; and Mine Mountain. Contrasts between these four mineralized areas illustrate the diverse nature of hydrothermal systems associated with the development of the SWNVF.

Geology of the SWNVF

The SWNVF is composed predominantly of silicic ash-flow tuff, including twelve sheets of regional extent, along with related surge and air-fall deposits and subordinate silicic to mafic lavas and intrusions. These rocks overlie complexly deformed and locally metamorphosed late Precambrian and Paleozoic miogeoclinal sedimentary rocks. Rocks of the SWNVF are distinctly younger than late Oligocene to early Miocene volcanic rocks exposed to the north (such as the volcanic rocks of the Goldfield district). Most rocks of the SWNVF were erupted between 15 and 10 Ma during the development of a large central complex of nested and overlapping volcanic centers of the collapse caldera type (Fig. 1). From about 9 to 7 Ma, volcanism in the SWNVF shifted to volcanic centers in the northwestern part of the field. Table 1 summarizes the stratigraphy and

TABLE 1

Generalized stratigraphy and geochronology of the southwestern Nevada volcanic field

Modified from Byers et al. (1989), Noble et al. (1991) and sources therein; additional age data from Hausback et al. (1990) and Sawyer et al. (1990); ages corrected for modern constants.

Formation	Member	Ma (approx.)	Volcanic Center
Late Magmatic Stage			
Stonewall Flat Tuff	Civet Cat Canyon	7.5	Stonewall Mountain caldera complex
	Spearhead	7.6	
Thirsty Canyon Tuff	Gold Flat	8.0	Black Mountain caldera complex
	Trail Ridge		
	Pahute Mesa		
	Rocket Wash	9.4	
Timber Mountain Magmatic Stage			
Rhyolite of Shoshone Mtn., Tuffs and lavas of the Bullfrog Hills		9-11	Periphery of Timber Mountain caldera complex
Mafic lavas		9-10	Timber Mountain caldera complex
Timber Mountain Tuff	Tuffs of Fleur de Lis Ranch	11.4	Timber Mountain caldera complex
	Ammonia Tanks	11.4	Timber Mtn. caldera complex - II
	Rainier Mesa	11.6	Timber Mtn. caldera complex - I
Rhyolite lavas of Fortymile Cyn.; pre-Rainier rhyolites		11-13	Timber Mountain caldera
Main Magmatic Stage			
Paintbrush Tuff	Tiva Canyon	12.7	Claim Canyon cauldron
	Yucca Mountain		Other members from area of
	Pah Canyon		Timber Mountain caldera complex
	Topopah Spring	13	
Rhyolite of Calico Hills		13	Calico Hills
Wahmonie & Salyer Fms.		13	Wahmonie
Crater Flat Tuff	Prow Pass		All members from Crater Flat—
	Bullfrog	13.1	Prospector Pass caldera
	Tram		complex (?)
Belted Range Tuff	Grouse Canyon	13.6	Silent Canyon caldera
Dacite lavas & breccias		14	Periphery of Crater Flat
Lithic Ridge Tuff		13.8	uncertain
Belted Range Tuff	Tub Spring	14.9	Silent Canyon caldera
"Older" tuffs			uncertain
Sanidine-rich tuff			uncertain
Tuff of Yucca Flat		15	uncertain
Redrock Valley Tuff		15.1	uncertain

geochronology of the three major magmatic stages of the SWNVF proposed by Noble et al. (1991): the 15.2–12.7-Ma main stage; the 11.6–9-Ma Timber Mountain stage; and the 9–7-Ma late stage.

Although the SWNVF is located within the Walker Lane structural belt, northwest-trending right-lateral faults and shear zones that characterize other parts of the belt are poorly developed in the SWNVF (Stewart, 1988). Instead, the majority of structural features within the SWNVF are attributed to magmatic and volcanic processes, including magmatic tumescence, caldera collapse and resurgent doming (Christiansen et al., 1977), and to middle- to late-Miocene regional extension that resulted in imbricate normal faulting and detachment faulting. In the southwestern part of the SWNVF, much extension appears to have been accommodated along the Original Bullfrog–Fluorspar Canyon (OB–FC) detachment fault system (Fig. 2), which is part of a regional fault system that continues southwest into Death Valley (Carr and Monsen, 1988; Hamilton, 1988).

Analytical methods

Chemical analyses were performed by Geochemical Services Inc., Rocklin, California, using inductively-coupled plasma emission spectroscopy (ICP-ES). Blind repeat analyses of sample pulps showed good reproducibility of results for all elements; but analyses on duplicate rock specimens show some differences (particularly for moderate- to high-level gold analyses) that are probably due to the "nugget effect". Comparative analyses done at the Nevada Bureau of Mines and Geology (NBMG) using atomic absorption for arsenic, bismuth, mercury and antimony showed excellent agreement for background-level samples collected from the SWNVF (Castor et al., 1990). Comparative analyses for gold, silver, arsenic and antimony performed by Bondar-Clegg, Inc., by instrumental neutron activation methods showed good agreement with the ICP-ES values for samples that ranged from background to highly mineralized. In addition, a comparison of Geochemical Services Inc., gold and silver values for NBMG standards (Lechler and Desilets, 1991) showed good agreement at high levels with recommended values obtained by averaging analyses by a number of commercial laboratories.

Mineral identifications were made using standard petrographic techniques, X-ray diffraction, and scanning electron microscope (SEM) analyses. Mineral compositions were obtained during SEM examination by energy dispersive X-ray (EDX) techniques using pure metal standards at the U.S. Bureau of Mines Western Research Center, Reno, Nevada. Mineral compositions reported are as molecular contents (rather than by weight percent). Descriptions of vein textures are based on a formal classification of the textures of vein quartz developed by Dowling and Morrison (1989).

Mineralized areas

Although records are sparse, we estimate that early gold production from the southern part of the SWNVF was about 3 t (100,000 oz) until significant operations ceased in the 1940s; silver production was of about the same magnitude. However, extensive exploration and development have taken place since the mid-1970s, and production and reserves for the SWNVF now total over 60 t (2 million oz) of gold and 150 t (5 million oz) of silver.

In connection with studies of mineral potential at the proposed nuclear waste site at Yucca Mountain, we obtained multi-element analyses of 150 vein and altered wall-rock samples from areas with precious-metal mineralization in the SWNVF. Our results (Table 2), together with data from the literature, show significant variations in trace-element suites for different mineralized areas in the SWNVF. For comparative purposes, analyses of unaltered volcanic

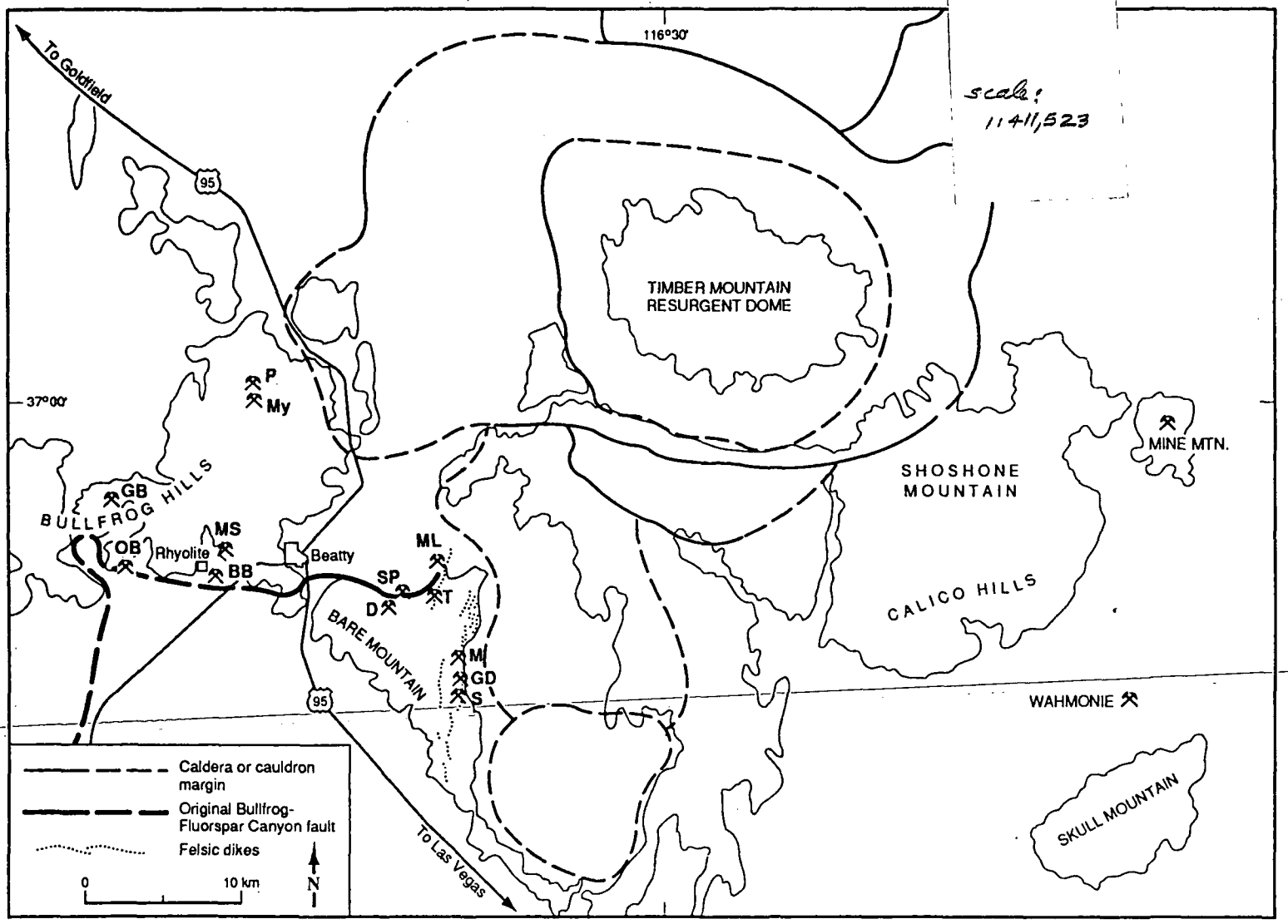

Fig. 2. Map of the south part of the southwestern Nevada volcanic field showing caldera margins, mineral deposits, and other features discussed in the text. (Modified from Noble et al., 1991.) *BB*=Lac Bullfrog mine, *D*=Daisy mine, *GB*=Gold Bar mine, *GD*=Goldspar mine, *M*=Mary mine, *ML*=Mother Lode mine, *MS*=Montgomery-Shoshone mine, *My*=Mayflower mine, *P*=Pioneer mine, *S*=Sterling mine, *SP*=Secret Pass deposit, *T*=Telluride mines. Heavy dashed line shows approximate surface trace of the Original Bullfrog–Fluorspar Canyon detachment fault system.

TABLE 2

Median, maximum and minimum trace-element contents of mineralized and altered samples from areas of precious-metal mineralization in the southwest Nevada volcanic field

Analyses by Geochemical Services, Inc.; all values in ppm, except Ag/Au; number of analyzed samples in parentheses.

	Ag			As			Au			Bi		
	Median	High	Low	Median	High	Low	Median	High	Low	Median	High	Low
Original Bullfrog (13)	1.79	1100	<.015	11.7	355	1.16	0.07	117	<.0005	<0.25	19.1	<0.25
Gold Bar (15)	0.39	30.8	0.05	3.02	8.7	1.05	0.07	3.76	0.006	<0.25	<0.25	<0.25
Rhyolite (42)	0.67	21000	<.015	6.8	88.2	<1.00	0.17	9223	<.0005	<0.25	0.52	<0.25
Mother Lode (36)	0.17	3.87	<.015	83.9	3874	1.63	0.05	7.47	0.001	<0.25	1.68	<0.25
Wahmonie (26)	0.48	3741	0.04	21.7	360	<1.00	0.01	383	<.0005	1.10	211	<0.25
Mine Mountain (21)	0.87	77.9	0.03	315	11200	<1.00	0.02	0.58	<.0005	<0.25	1.22	<0.25
	Cd			Cu			Ga			Hg		
	Median	High	Low	Median	High	Low	Median	High	Low	Median	High	Low
Original Bullfrog (13)	<0.10	1.42	<0.10	60.8	5160	21.8	<0.50	10.3	<0.50	<0.10	0.18	<0.10
Gold Bar (15)	<0.10	0.13	<0.10	24.4	47.8	2.48	0.96	5.11	<0.50	<0.10	0.46	<0.10
Rhyolite (42)	<0.10	0.42	<0.10	3.31	4413	0.92	0.53	2.2	<0.50	<0.10	1.22	<0.10
Mother Lode (36)	<0.10	1.03	<0.10	4.6	41.5	1.04	0.75	20	<0.50	0.25	5.87	<0.10
Wahmonie (26)	<0.10	0.27	<0.10	18.7	2434	2.24	0.51	1.66	<0.50	0.16	59.6	<0.10
Mine Mountain (21)	6.34	864	<0.10	35.6	531	2.31	0.88	9.23	<0.50	8.28	624	0.21
	Mo			Pb			Sb			Se		
	Median	High	Low	Median	High	Low	Median	High	Low	Median	High	Low
Original Bullfrog (13)	3.2	8.5	1.8	9	91.3	2.3	2.2	494	0.3	<1.0	<1.0	<1.0
Gold Bar (15)	2.1	3.7	0.5	9.2	17.6	1.3	0.5	1.0	<0.25	<1.0	<1.0	<1.0
Rhyolite (42)	4.4	429	1.2	8.6	381	0.6	0.7	296	<0.25	<1.0	173	<1.0
Mother Lode (36)	3.8	45.2	0.4	6.9	93.7	0.6	6.3	2077	<0.25	<1.0	8.3	<1.0
Wahmonie (26)	3.5	16.4	0.5	7.7	205	1.1	1.3	9.9	<0.25	<1.0	3.7	<1.0
Mine Mountain (21)	4.6	324	0.3	268	23k	1.9	181	2920	<0.25	<1.0	34.7	<1.0
	Te			Tl			Zn			Ag/Au		
	Median	High	Low	Median	High	Low	Median	High	Low	Median	High	Low
Original Bullfrog (13)	<0.5	5.0	<0.5	<0.5	4.5	0.5	24.7	125	2.1	22.7	216	6.4
Gold Bar (15)	<0.5	<0.5	<0.5	<0.5	<0.5	<0.5	19.3	34.4	2.8	8.19	33.1	1.0
Rhyolite (42)	<0.5	12	<0.5	<0.5	4.5	<0.5	15.8	179	2.7	2.3	87	0.37
Mother Lode (36)	<0.5	5.2	<0.5	<0.5	5.2	<0.5	11.6	261	<1.0	1.67	220	0.1
Wahmonie (26)	1.5	90.4	<0.5	<0.5	2.7	<0.5	7.1	61.5	<1.0	37.5	227	2.86
Mine Mountain (21)	<0.5	0.8	<0.5	<0.5	1.5	<0.5	705	146k	1.5	17.4	30k	2.73

TABLE 3

Trace-element analyses of background samples from the southwestern Nevada volcanic field

Analyses by Geochemical Services, Inc.; all values in ppm, except for Au which is in ppb; no data reported for Hg, Bi, Tl, and tellurium, which are below detection levels of 0.1, 0.25, 0.5, and 0.5 ppm, respectively.

SAMPLE	Ag	As	Au	Cu	Mo	Pb	Sb	Zn	Cd	Ga	Se
Glassy tuff											
SC 12	0.023	<1.0	1.0	5.3	0.6	4.9	<0.25	24.9	0.26	<0.50	<1.0
SC 16	0.021	<1.0	<0.5	5.6	0.7	2.8	<0.25	20.0	0.10	0.5	<1.0
SC 93	<0.015	<1.0	1.0	1.0	0.2	2.4	<0.25	17.6	<0.10	1.0	<1.0
SC 46A	0.017	<1.0	1.0	4.5	0.4	4.9	<0.25	12.0	0.16	<0.50	<1.0
BH 34G	0.044	1.9	<0.5	2.2	1.2	5.1	<0.25	11.4	<0.10	1.5	<1.0
BH 40	0.037	1.5	<0.5	1.0	0.8	5.7	<0.25	6.6	<0.10	1.2	<1.0
BH 43	0.034	2.4	<0.5	0.9	1.1	6.7	<0.25	8.2	<0.10	1.6	<1.0
Devitrified tuff											
SC 11	0.021	1.1	<0.5	14.3	1.7	5.1	<0.25	29.9	<0.10	<0.50	<1.0
SC 15	0.028	2.6	1.0	10.1	1.4	9.1	<0.25	35.2	<0.10	<0.50	<1.0
SC 23	0.034	1.4	2.0	15.5	1.8	5.1	<0.25	27.8	<0.10	<0.50	<1.0
SC 48C	0.027	1.3	1.0	10.2	1.2	1.2	<0.25	30.7	<0.10	1.0	<1.0
SC 58	0.029	2.8	<0.5	11.8	1.4	2.9	<0.25	20.5	<0.10	0.8	<1.0
SC 64	0.021	2.2	<0.5	12.3	1.3	9.2	<0.25	19.1	<0.10	0.8	<1.0
SC 80	0.028	2.2	<0.5	2.5	1.7	2.0	1.5	31.9	0.14	0.8	<1.0
DD 42	0.020	2.2	<0.5	1.6	1.2	1.7	<0.25	30.2	<0.10	<0.50	<1.0
DD 54	0.027	1.6	1.0	3.9	1.6	4.4	<0.25	12.2	<0.10	1.0	<1.0
DD 55 A	0.018	6.2	<0.5	3.5	1.0	2.0	<0.25	28.5	0.13	0.6	<1.0
DD 55 B	<0.015	1.3	1.0	3.9	1.1	1.8	<0.25	7.4	<0.10	0.6	<1.0
BH 34	0.035	3.9	<0.5	1.5	1.0	9.9	<0.25	33.7	<0.10	1.5	<1.0
BH 35	0.053	9.2	<0.5	1.8	1.1	8.4	<0.25	19.6	<0.10	2.0	<1.0
BH 41	0.052	3.9	<0.5	1.8	1.9	6.6	<0.25	10.8	<0.10	1.4	<1.0
BH 32	0.031	2.7	1.0	2.2	0.7	8.0	<0.25	26.7	0.15	2.5	1.1
BH 33	0.037	2.9	1.0	2.2	1.2	12.0	<0.25	9.5	<0.10	1.5	<1.0
GEXA 50	0.032	2.2	3.0	28.6	2.8	4.8	0.42	38.1	<0.10	3.2	<1.0
Volcanic sediment											
GEXA 20	0.025	14.0	2.0	5.4	1.2	17.7	<0.25	32.2	0.05	<0.50	<1.0

Glassy tuff	
SC 12	Orange glassy ash-flow tuff, bedded tuff unit, Yucca Mtn.
SC 16	Gray glassy ash-flow tuff, bedded tuff unit, Yucca Mtn.
SC 93	Gray glassy ash-flow tuff, bedded tuff unit, Yucca Mtn.
SC 46A	Black vitrophyre, Tiva Canyon Mbr., Yucca Mtn.
BH 34G	Brown glassy ash-flow tuff, Tiva Canyon Mbr., Bullfrog Mtn.
BH 40	Brown and black vitrophyre, Rainier Mesa Mbr., Bullfrog Mtn.
BH 43	Brown vitrophyre, Ammonia Tanks Mbr., Paradise Mtn.
Devitrified tuff	
SC 11	Lithophysal ash-flow tuff, Topopah Spring Mbr., Yucca Mtn.
SC 15	Clinkstone ash-flow tuff, Tiva Canyon Mbr., Yucca Mtn.
SC 23	Columnar ash-flow tuff, Tiva Cyn. Mbr., Yucca Mtn.
SC 48C	Brown biotitic ash-flow tuff, Topopah Spring Mbr., Yucca Mtn.
SC 58	Lithophysal ash-flow tuff, Topopah Spring Mbr., Yucca Mtn.
SC 64	Crystal-rich ash-flow tuff, Rainier Mesa Mbr., Yucca Mtn.
SC 80	Red-brown ash-flow tuff, Topopah Spr. Mbr., Yucca Mtn.
DD 42	Lithophysal ash-flow tuff, Tiva Canyon Mbr., Yucca Mtn.
DD 54	Crystal-rich ash-flow tuff, Rainier Mesa Mbr., Yucca Mtn.
DD 55 A	Crystal-rich ash-flow tuff, Rainier Mesa Mbr., Yucca Mtn.
DD 55 B	Air-fall tuff below Rainer Mesa Mbr., Yucca Mtn.
BH 34	Pinkish-grey ash-flow tuff, Tiva Canyon Mbr., Bullfrog Mtn.
BH 35	Pink ash-flow tuff, Crater Flat Tuff, Bullfrog Mtn.
BH 41	Brown ash-flow tuff, Rainier Mesa Mbr., Bullfrog Mtn.
BH 32	Light gray air-fall(?) tuff, Rainier Mesa Mbr., Bullfrog Mtn.
BH 33	Light gray air-fall(?) tuff, Rainier Mesa Mbr., Bullfrog Mtn.
GEXA 50	Flow(?) rock, rocks of Joshua Hollow, E of Mother Lode mine
Volcanic sediment	
GEXA 20	Fine sandstone, rocks of Joshua Hollow, SE of Mother Lode mine

MOTHER LODE MINE

	Ag	As	Au	Bi	Cd	Cu	Ga	Hg	Mo	Pb	Sb	Se	Te	Tl	Zn
Ag	1.00														
As	0.62√	1.00													
Au	0.72√	0.62√	1.00												
Bi	-0.28	-0.04	-0.01	1.00											
Cd	0.46√	0.43√	0.27	-0.14	1.00										
Cu	0.48√	0.67√	0.52√	-0.13	0.37	1.00									
Ga	-0.16	0.17	-0.07	0.17	-0.16	-0.12	1.00								
Hg	0.29	0.43√	0.34	0.18	0.39	0.40√	-0.22	1.00							
Mo	-0.08	0.04	-0.14	0.14	0.27	0.30	-0.09	0.27	1.00						
Pb	0.59√	0.67√	0.50√	0.17	0.24	0.47√	0.20	0.28	0.05	1.00					
Sb	0.63√	0.88√	0.65√	0.00	0.52√	0.61√	0.06	0.51√	0.10	0.71√	1.00				
Se	0.22	0.54√	0.25	0.23	0.42√	0.48√	0.25	0.26	0.35	0.47√	0.43√	1.00			
Te	0.62√	0.54√	0.58√	-0.10	0.40√	0.33	0.18	0.34	0.07	0.54√	0.66√	0.22	1.00		
Tl	0.61√	0.51√	0.56√	-0.08	0.31	0.35	0.16	0.30	-0.02	0.51√	0.62√	0.05	0.80√	1.00	
Zn	0.44√	0.65√	0.28	-0.28	0.69√	0.64√	-0.04	0.46√	0.30	0.37√	0.64√	0.41√	0.33	0.40√	1.00

ORIGINAL BULLFROG MINE

	Ag	As	Au	Bi	Cd	Cu	Ga	Hg	Mo	Pb	Sb	Se	Te	Tl	Zn
Ag	1.00														
As	0.33	1.00													
Au	0.88√	0.28	1.00												
Bi	0.59	0.51	0.42	1.00											
Cd	0.61	0.89√	0.53	0.54	1.00										
Cu	0.82√	0.54	0.54	0.74√	0.63	1.00									
Ga	0.59	-0.02	-0.59	-0.58	-0.18	-0.66√	1.00								
Hg	-0.51	-0.06	-0.47	-0.47	-0.11	-0.65√	0.80√	1.00							
Mo	0.23	0.56	0.12	0.47	0.57	0.34	-0.18	-0.05	1.00						
Pb	0.14	0.76√	0.00	0.49	0.62	0.24	0.30	0.25	0.35	1.00					
Sb	0.92√	0.50	0.91√	0.21	0.71√	0.78√	-0.45	-0.50	0.21	0.24	1.00				
Se												1.00			
Te	0.08	0.00	-0.16	0.08	0.08	0.08	-0.25	-0.16	0.46	-0.23	-0.16		1.00		
Tl	-0.23	0.10	-0.30	0.09	0.07	-0.13	0.08	0.22	0.76√	0.02	-0.27		0.41	1.00	
Zn	-0.42	0.57	-0.44	-0.19	0.32	-0.21	0.63	0.50	0.42	0.58	-0.21		-0.08	0.38	1.00

WAHMONIE DISTRICT

	Ag	As	Au	Bi	Cd	Cu	Ga	Hg	Mo	Pb	Sb	Se	Te	Tl	Zn
Ag	1.00														
As	0.11	1.00													
Au	0.84√	0.28	1.00												
Bi	0.51√	0.32	0.47√	1.00											
Cd	0.49√	0.41	0.38	0.22	1.00										
Cu	0.21	0.24	0.07	0.47√	0.22	1.00									
Ga	-0.23	0.51√	0.09	0.03	-0.10	0.08	1.00								
Hg	0.69√	0.04	0.62√	0.43	0.51√	0.29	-0.14	1.00							
Mo	-0.16	0.16	-0.02	-0.02	-0.16	0.05	0.50√	0.14	1.00						
Pb	0.07	0.44	0.06	0.70√	0.18	0.34	0.25	0.13	0.18	1.00					
Sb	-0.01	0.74√	0.15	0.12	0.24	0.23	0.25	0.10	0.17	0.30	1.00				
Se	-0.16	0.46√	-0.16	0.19	-0.05	-0.06	0.32	-0.10	0.24	0.36	0.14	1.00			
Te	0.72√	0.38	0.68√	0.75√	0.30	0.32	-0.04	0.58√	-0.03	0.49√	0.28	0.03	1.00		
Tl	0.33	0.31	0.33	0.28	0.41	0.28	0.30	0.35	0.33	0.28	0.31	-0.13	0.34	1.00	
Zn	0.25	0.32	0.32	0.15	0.52√	0.28	0.12	0.40	-0.06	0.26	0.43	-0.32	0.42	0.33	1.00

GOLD BAR MINE

	Ag	As	Au	Bi	Cd	Cu	Ga	Hg	Mo	Pb	Sb	Se	Te	Tl	Zn
Ag	1.00														
As	-0.26	1.00													
Au	0.60√	0.29	1.00												
Bi				1.00											
Cd	-0.37	-0.25	-0.25		1.00										
Cu	0.31	0.41	0.63√		-0.25	1.00									
Ga	-0.06	0.31	0.31		0.31	0.22	1.00								
Hg	-0.09	0.77	0.48		-0.18	0.71√	0.30	1.00							
Mo	0.09	0.29	0.22		-0.37	0.37	-0.31	0.40	1.00						
Pb	-0.38	0.65√	0.08		-0.22	0.28	-0.17	0.66√	0.72√	1.00					
Sb	-0.19	0.43	0.29		0.22	0.25	0.50	0.49	0.04	0.38	1.00				
Se												1.00			
Te													1.00		
Tl														1.00	
Zn	-0.69√	0.40	-0.26		0.40	-0.21	0.69√	0.13	-0.24	0.13	0.35				1.00

MINE MOUNTAIN

	Ag	As	Au	Bi	Cd	Cu	Ga	Hg	Mo	Pb	Sb	Se	Te	Tl	Zn
Ag	1.00														
As	0.65√	1.00													
Au	0.55√	0.78√	1.00												
Bi	-0.13	-0.10	-0.04	1.00											
Cd	0.90√	0.68√	0.52√	-0.20	1.00										
Cu	0.47	0.45	0.58√	0.00	0.52√	1.00									
Ga	-0.22	0.00	0.03	-0.03	-0.28	-0.21	1.00								
Hg	0.90√	0.66√	0.43	-0.20	0.85√	0.44	-0.19	1.00							
Mo	0.23	0.16	0.06	-0.19	0.09	-0.22	0.17	0.23	1.00						
Pb	0.93√	0.72√	0.56√	-0.18	0.88√	0.40	-0.29	0.86√	0.26	1.00					
Sb	0.83√	0.69√	0.54√	-0.08	0.79√	0.29	-0.18	0.74√	0.33	0.92√	1.00				
Se	0.42	0.72√	0.68√	0.04	0.46	0.45	0.03	0.37	0.03	0.46	0.45	1.00			
Te	0.13	0.19	-0.02	-0.10	0.13	-0.14	0.47	0.12	0.22	0.10	0.07	0.23	1.00		
Tl	-0.04	0.19	0.03	-0.16	-0.14	-0.37	0.34	-0.01	0.38	0.02	-0.15	0.06	0.33	1.00	
Zn	0.79√	0.65√	0.37	-0.28	0.92√	0.44	-0.22	0.83√	0.19	0.79√	0.65√	0.47	0.33	0.06	1.00

RHYOLITE AREA

	Ag	As	Au	Bi	Cd	Cu	Ga	Hg	Mo	Pb	Sb	Se	Te	Tl	Zn
Ag	1.00														
As	0.05	1.00													
Au	0.76√	0.09	1.00												
Bi	0.27	-0.01	0.22	1.00											
Cd	0.22	0.21	0.01	0.12	1.00										
Cu	0.47√	0.38√	0.37√	0.24	0.26	1.00									
Ga	0.35	0.52√	-0.29	-0.30	-0.24	-0.06	1.00								
Hg	0.20	0.09	0.21	-0.10	-0.06	-0.02	0.14	1.00							
Mo	0.26	-0.07	0.02	0.17	0.34	-0.19	-0.31	-0.05	1.00						
Pb	-0.12	0.41√	-0.17	0.18	0.25	0.19	0.19	-0.13	-0.06	1.00					
Sb	0.28	0.65√	0.10	0.28	0.28	0.48√	0.19	0.00	0.02	0.25	1.00				
Se	0.37√	0.29	0.36√	0.28	0.30	0.25	-0.03	0.05	0.28	0.06	0.21	1.00			
Te	0.42√	-0.06	0.44√	0.48√	0.22	0.27	-0.21	0.17	0.01	0.29	-0.02	0.40√	1.00		
Tl	0.31	-0.17	0.11	0.43√	0.51√	0.18	-0.46√	-0.15	0.34	-0.01	0.22	0.25	0.17	1.00	
Zn	-0.08	0.58√	-0.16	-0.05	0.47√	0.10	0.36√	0.06	0.16	0.32	0.24	0.18	0.00	0.07	1.00

√ Correlation coefficient significant at 99% confidence level

√ Correlation coefficient significant at 99% confidence level

Fig. 3. Spearman correlation coefficients for trace-element analyses in samples from mineralized areas in the southwestern Nevada volcanic field.

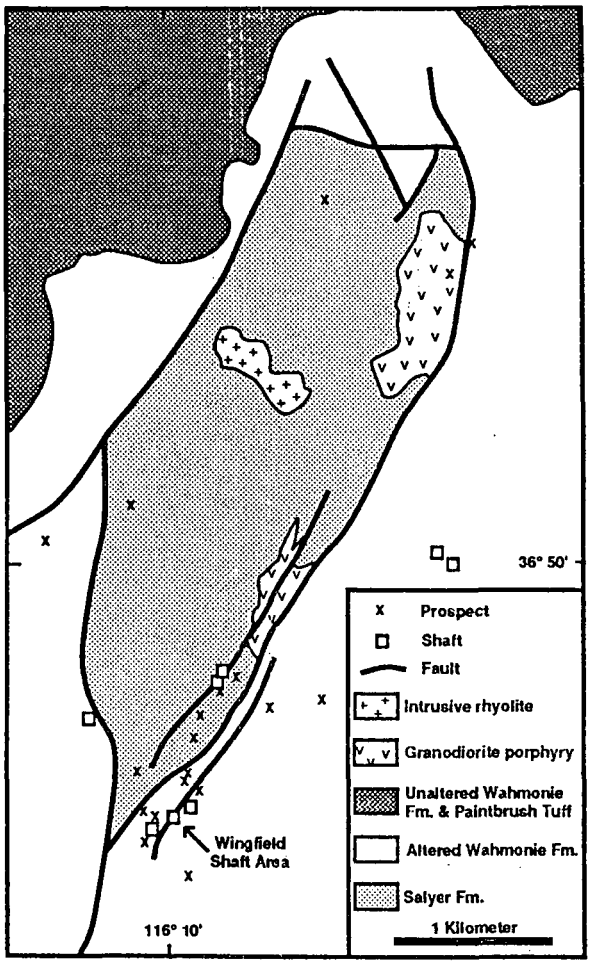

Fig. 4. Map showing mine workings and generalized geology for part of the Wahmonie district. (Modified from Ekren and Sargent, 1965.)

rocks from the SWNVF are also reported (Table 3). Correlation coefficients between trace-element contents for each area represented by thirteen or more samples are shown in Fig. 3.

We have not separated the chemical data reported in this study (Table 2) by sample type (e.g., vein versus wall rock) because few samples composed exclusively of vein or wall-rock material were analyzed. Most samples consisted of variable proportions of mixed vein and altered wall-rock material, or of disseminated mineralization containing little or no vein material. In addition, analyses of the few pure vein and wall-rock samples showed little difference in trace-element assemblage other than overall metal concentration. Most of the samples collected during this study are partially to completely oxidized. In a few cases where unoxidized samples could be compared with oxidized samples from the same locality, trace-element signatures were not found to be significantly different. The data presented here reflect differences in trace-element signatures between mineralized areas that are more significant than differences within areas.

Wahmonie district

The earliest mining activity in rocks of the SWNVF took place in the Wahmonie mining district (Figs. 2 and 4) where near-surface ores are thought to have been worked as early as 1853 (Quade et al., 1984). Discoveries of high-grade silver-gold ore in 1928 resulted in considerable development, including the 150-m-deep Wingfield shaft, but little ore was shipped. In 1940, the Wahmonie district was withdrawn from mineral entry when it was included within the Tonopah Bombing and Gunnery Range. This area later became part of the Nevada Test Site of the U.S. Department of Energy and remains excluded from civilian development.

Precious-metal mineralization in the Wahmonie district lies in a northeast-trending 8 km by 4 km elliptical area underlain by intensely altered andesitic to latitic lavas, tuffs and breccias of the Wahmonie Formation (Ekren and Sargent, 1965). The altered area includes a central northeast-trending 3 km by 1 km horst, containing weakly to strongly altered rhyodacitic volcanic rocks assigned to the Salyer Formation (Ekren and Sargent, 1965), that are cut by intermediate to silicic subvolcanic intrusions (Fig. 4). The intermediate to felsic igneous rocks at Wahmonie probably comprise the eroded remnants of a central volcano or dome and flow field. K/Ar ages (recalculated to current constants) indicate that rocks comprising this center, informally termed the

Wahmonie–Salyer volcanic center, were emplaced between about 13.2 and 12.8 Ma (Kistler, 1968). They are overlain by units of the Paintbrush Tuff (Ekren and Sargent, 1965), which have similar to slightly younger ages of about 13.0 to 12.7 Ma (Sawyer et al., 1990).

The area of the most intense prospecting and development, which includes the Wingfield shaft (Fig. 4), is a northeast-trending zone of abundant quartz veins, about 1 km long in strongly altered rock along the southeastern side of the central horst. Near-vein alteration in this area is dominated by silicification and adularization with some argillic minerals. Feldspar phenocrysts are replaced by granular adularia with illite + sericite ± kaolinite or by single crystals of secondary potash feldspar with mottled extinction. According to Jackson (1988), near-vein adularia + sericite + silica alteration grades outward to kaolinite-bearing rock. Alunite was reported to occur in strongly altered rock and in quartz veins (Ekren and Sargent, 1965; Quade et al., 1984), but no alunite was found by the authors during petrographic and X-ray diffraction analyses. Sulfide-rich silicified rock on mine dumps in the Wingfield shaft area, and widespread limonite indicate that significant amounts of pyrite were previously present in altered wall rock. Propylitic alteration consisting of chlorite ± albite ± calcite ± pyrite is widespread in the central horst. Argillic alteration, potassic alteration (with secondary biotite), and tourmaline veinlets are locally present in, or adjacent to, central horst intrusions.

Precious-metal-bearing veins consist mainly of fine comb quartz ± calcite with minor adularia. They carry free gold, cerargyrite, hessite, iron and manganese oxides, acanthite and other sulfides (Quade et al., 1984). Very finely granular quartz veins with anomalously high precious-metal contents (as much as 0.4 ppm gold and 3.5 ppm silver) are exposed in the vicinity of the Wingfield shaft. Stockworks of fine comb to granular quartz veinlets with adularia rhombs are also present.

SEM/EDX studies of highly mineralized rock from Wahmonie disclosed electrum ($Au_{77}Ag_{23}$) occurring as irregular threads or flakes in cerargyrite, and hessite (Ag_2Te) occurring as colloform bands in cerargyrite. Iron tellurite containing minor gold and manganese (possibly mackayite, $Fe_2(TeO)_3 \cdot x\ H_2O$) was found in cerargyrite. Frohbergite ($FeTe_2$) and hedleyite ($BiTe_2$) were also tentatively identified, and cinnabar was found in cavities as micron-size granules on cerargyrite (J. Sjoberg and J. Quade, pers. commun., 1991).

Vein samples analyzed during this study contain as much as 3.7 kg silver and 0.4 kg gold per ton, but samples carrying as much as 38.7 kg silver and 1.7 kg gold per ton have been reported previously (Quade et al., 1984). Mineralized and altered samples from the Wahmonie district have relatively high silver:gold ratios (Table 2) and bismuth, mercury and tellurium correlate well with gold (Figs. 3 and 5). Copper, lead and antimony are locally high, but do not correlate with gold. Base-metal contents are low in mineralized samples from Wahmonie, with the exception of a single vein sample with secondary copper minerals that is enriched in copper and lead, but poor in silver and gold. Arsenic content is generally low (Table 2), but pyrite-rich silicified rock with 360 ppm arsenic was collected from a dump near the Wingfield shaft.

Rock with high precious-metal and tellurium contents in the Wahmonie district is not restricted to the Wingfield shaft area, and may occur widely in the district. Hessite-bearing comb quartz from a small dump in the central horst, 1 km northeast of the Wingfield shaft, contains 748 ppm silver, 11 ppm gold and 90 ppm tellurium. Granodiorite, altered to a mixture of quartz and illite (4 km northeast of the Wingfield shaft), also has elevated gold and tellurium contents (Quade et al., 1984).

Adularia from altered rocks with abundant silica-adularia veins in the Wahmonie district gave K/Ar ages of 12.6 ± 0.4 and 12.9 ± 0.4 Ma (Jackson, 1988). These ages indicate that hy-

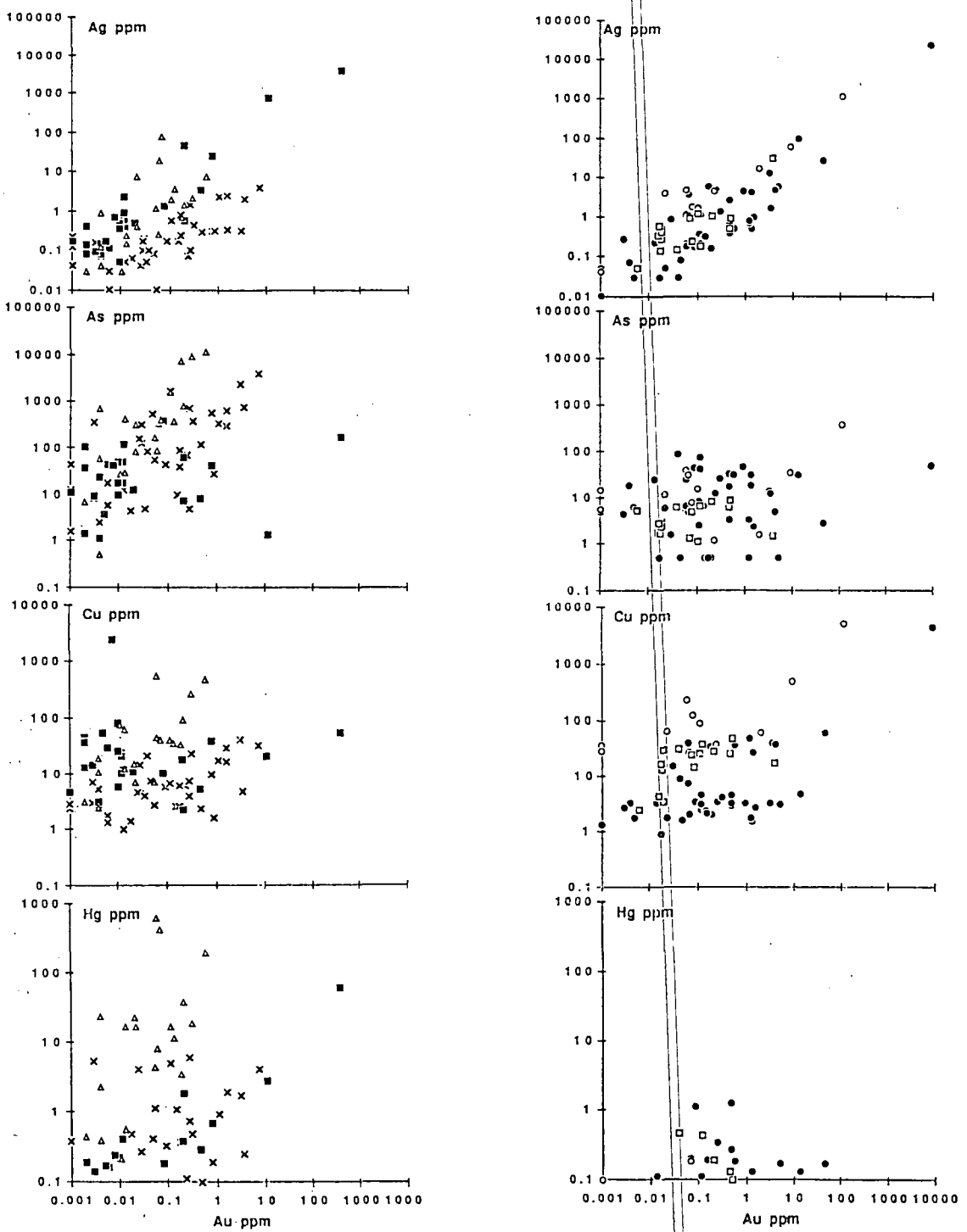

Fig. 5. Plots of Ag, As, Hg and Cu against Au in samples from mineralized areas in the southwestern Nevada volcanic field. Plots on the left represent samples from Wahmonie (■) Bare Mountain (×), and Mine Mountain (△). Plots on the right are of samples from the Bullfrog mining district: Original Bullfrog mine (⊙); Gold Bar mine (□); and Rhyolite area (●).

drothermal activity and mineralization closely followed magmatic and volcanic activity of the main magmatic stage of the SWNVF at Wahmonie.

On the basis of a positive residual gravity anomaly centered about 1 km southwest of the mineralized area at Wahmonie and associated magnetic highs, Ponce (1981) inferred the presence of a large buried felsic intrusive mass similar to and contiguous with granodiorite exposures in the central horst. The highest portions of this intrusive body appear to be along the east side of the central horst, coincident with the area of precious-metal mineralization. As pointed out by Hoover et al. (1982), the edges of the inferred intrusion correspond approximately with alteration in the Wahmonie district. Relatively high resistivity in the inferred intrusion indicates high porosity due to fracturing, faulting, alteration and possibly mineralization. Induced polarization data indicate that 2% or more sulfides are present below the water table at Wahmonie (Hoover et al., 1982).

Alteration and veining in granodioritic porphyry intrusions in the central horst, along with high bismuth and tellurium support the presence of a porphyry magmatic–hydrothermal system at Wahmonie. In addition, quartz phenocrysts containing hypersaline secondary fluid inclusions, which are indicative of magmatic hydrothermal fluids, occur in samples with secondary biotite (D.C. Noble, pers. commun., 1990).

Bare Mountain area

Between initial discovery in 1905 and the late 1970s, small amounts of gold and mercury were produced intermittently from deposits in northern and eastern Bare Mountain, including the Panama-Sterling gold mine and the Telluride gold-mercury camp (Fig. 2). Fluorspar was produced more-or-less continuously from the same area between 1918 and 1989 from the Daisy, Goldspar and Mary mines. Approximately 2.5 t (80,000 oz) of gold were produced from disseminated deposits at the Sterling and Mother Lode mines between 1983 and 1990 (Bonham and Hess, 1991). Additional, currently subeconomic disseminated gold deposits are present at the Daisy mine, Secret Pass, Goldspar mine, and near the Mother Lode mine (J. Marr, pers. commun., 1987; Greybeck and Wallace, 1991).

Bare Mountain consists predominantly of weakly metamorphosed late Proterozoic through late Paleozoic sedimentary rocks of the Cordilleran miogeocline that underwent Mesozoic folding and thrust-faulting and Tertiary low- to high-angle normal and strike-slip faulting (Cornwall and Kleinhampl, 1961; Monsen et al., 1990). In northern Bare Mountain, these rocks are separated from overlying, imbricately faulted volcanic rocks of the SWNVF by the north-dipping, low- to moderate-angle Fluorspar Canyon fault (Cornwall and Kleinhampl, 1961) which is considered by recent workers to be the eastern continuation of the Original Bullfrog fault (e.g., Carr and Monsen, 1988). In contrast to the Bullfrog Hills, where major faulting and tilting post-dated deposition of the 11.4 Ma Ammonia Tanks Member, deformation in northeastern Bare Mountain had mostly ceased by 11.6 Ma, as indicated by strong angular discordance between the flat-lying, 11.6-Ma Rainier Mesa Member of the Timber Mountain Tuff and underlying tilted units of the SWNVF (Carr, 1984; Carr and Monsen, 1988; Monsen et al., 1990; Weiss et al., 1990).

A swarm of north-trending felsic porphyry dikes intrudes the pre-Cenozoic rocks in eastern and northern Bare Mountain. The dike rocks typically have coarsely granophyric groundmass and have been affected by variable degrees of potassium-feldspar, sericitic and argillic alteration. Secondary hypersaline fluid inclusions that are present in quartz phenocrysts reflect the passage of an early high-salinity hydrothermal fluid (Noble et al., 1989). The dikes were emplaced during the

main magmatic stage of the SWNVF, as demonstrated by radiometric age determinations ranging between 14.9±0.5 and 13.8±0.2 Ma (Marvin et al., 1989; Monsen et al., 1990; Noble et al., 1991). Most mineral deposits along the east flank of Bare Mountain are spatially associated with, and post-date or are nearly contemporaneous with the emplacement of, these dikes.

Several base-metal±gold occurrences, generally associated with quartz veins in Precambrian and Cambrian rocks, have been reported along the west flank of Bare Mountain (Cornwall, 1972; Tingley, 1984). However, most of the mineral deposits in Bare Mountain are located in its northern and eastern flanks.

At the Sterling mine (Fig. 2), sediment-hosted disseminated gold-silver mineralization is controlled by the intersection of normal faults with a thrust fault that juxtaposes clastic rocks of the late Proterozoic to early Cambrian Wood Canyon Formation over carbonate rocks of the middle Cambrian Bonanza King Formation (Odt, 1983). This mineralization is associated with alteration assemblages that include kaolinite, illite, sericite, jarosite and alunite, and with very little introduction or removal of silica and iron (Odt, 1983). Stibnite, cinnabar and fluorite are present in ore and in nearby exposures of hydrothermal breccia (Tingley, 1984). Hydrothermally altered porphyry dikes are abundant in the Sterling Mine area, and locally have elevated gold contents (Odt, 1983; Tingley, 1984; Jackson, 1988).

North of the Sterling mine, a zone of argillic alteration and bleaching accompanies the porphyry dikes and locally contains fluorite and disseminated gold mineralization in Paleozoic carbonate rocks (Tingley, 1984; D. Odt, pers. comm., 1987). At the Goldspar mine (Fig. 2), fluorite replaces brecciated and sheared carbonate rocks of the Nopah Formation and fills fractures in altered dike rock (Papke, 1979; Tingley, 1984; Jackson, 1988). Similar fluorite mineralization and alteration is present in Silurian dolomite at the Mary mine.

The Goldspar deposit has been interpreted as a high-level breccia pipe (e.g., Tingley, 1984). Altered clasts of Tertiary volcanic rocks in the breccia (Jackson, 1988) are unlikely to have been transported from below the Cambrian host rocks. This suggests that the breccia was open to much higher stratigraphic levels at the time of hydrothermal activity.

In the Telluride mine area (Fig. 2), gold mineralization is present with quartz, opal, alunite and pyrite along the Fluorspar Canyon fault (Jackson, 1988) and occurs in altered porphyry dikes that intrude carbonate rocks in the footwall of the fault. Mercury was mined from pipe-like breccia bodies and also occurs as disseminated cinnabar with fluorite, calcite, opal and alunite at the Telluride mine (Tingley, 1984).

The Mother Lode gold mine is situated immediately to the north of the Telluride mine area, near the northeasternmost exposure of the Fluorspar Canyon fault segment of the OB-FC fault system (Fig. 2). Disseminated gold mineralization is present in felsic porphyry dikes, sills and extrusive(?) rocks and in adjacent interbedded sandstone, siltstone and limestone. Mapa (1990) considered the sedimentary host rocks to be part of the Mississippian Eleana Formation, whereas others (e.g., S. Ristorcelli, pers. commun., 1990) interpret them as belonging to the early(?) to middle Miocene rocks of Joshua Hollow of Monsen et al. (1990). Alteration is primarily argillic, with pyrite in unoxidized rocks and jarosite in oxidized rocks. Altered rock is mostly composed of quartz and illite, and feldspar phenocrysts are generally completely replaced by illite±calcite, but some samples contain sanidine that is apparently unaltered. Mafic minerals are replaced by sericite±illite±calcite ±rutile. Sooty remobilized carbon is abundant locally in the sedimentary rocks. Very sparse, irregular veins containing fine to medium drusy quartz+ manganese oxide±opal occur in oxidized ore, and calcite veins cut limestone. About 150 m west of the mine,

glassy bedded tuff that is considered to lie stratigraphically between the Paintbrush and Timber Mountain Tuffs (Monsen et al., 1990) contains very fine-grained alunite. In addition, chalcedony replaces conglomerate and opal replaces bedded tuff in the same unit about 600 m northwest of the mine.

Three mineralized zones, containing a total of 12.3 Mt that average 0.81 g/t of gold (13.5 Mst at 0.026 oz/st), have been delineated in Fluorspar Canyon 3–5 km southwest of the Mother Lode mine (Greybeck and Wallace, 1991). In this area, two disseminated gold deposits associated with fluorite mineralization are present within Cambrian rocks of the Nopah, Bonanza King and Carrara Formations in and near the Daisy fluorite mine (Fig. 2) (Papke, 1979; Tingley, 1984; Greybeck and Wallace, 1991). These deposits, which are situated beneath the Fluorspar Canyon fault (Fig. 2), are associated with alteration that ranges from subtle decalcification to intense silicification (Greybeck and Wallace, 1991). Cinnabar commonly accompanies fluorite in the Daisy mine.

The nearby volcanic-hosted Secret Pass deposit (Fig. 2) contains disseminated gold in altered ash-flow tuff of the Bullfrog Member of the Crater Flat Tuff. The deposit is bounded by the underlying Fluorspar Canyon fault (Greybeck and Wallace, 1991). An alteration assemblage including quartz, adularia, calcite and pyrite, with generally weak silicification, is associated with gold mineralization (Greybeck and Wallace, 1991). Although precious-metal mineralization is confined to the Crater Flat Tuff, adularia- and illite(?)-bearing alteration assemblages continue up into the overlying ca. 13-Ma Topopah Spring Member of the Paintbrush Tuff. In addition, chalcedonic veins that may be related to this mineralization are present in the 12.7-Ma Tiva Canyon Member.

Altered and mineralized samples from the Bare Mountain area collected during this study include twenty samples from the Mother Lode orebody and sixteen samples from workings and outcrops within 1 km south and west of the mine. These samples generally have high arsenic and antimony contents, and gold correlates strongly with these two elements (Figs. 2 and 5). Gold is also correlative with copper, lead, mercury, tellurium and thallium, although the contents of these metals are not highly anomalous. The median silver:gold ratio for all 36 samples is about 2:1. In general, Mother Lode mine samples with the highest gold contents contain drusy quartz ± opal along with manganese oxide. Pyritic ore contains gold contents similar to adjacent oxidized ore (W. Hickinbotham, pers. commun., 1990). Gold-bearing phases could not be found using reflected light and scanning electron microscopy in samples containing as much as 7 ppm gold.

The mineralized areas in Fluorspar Canyon southwest of the Mother Lode mine have similar trace-element abundances and correlations between gold and other trace elements, particularly antimony, thallium, and molybdenum (Greybeck and Wallace, 1991). Arsenic, mercury and base metals are also correlative with gold, but not in all three deposits. Silver:gold ratios are generally low.

Gold-rich samples from the Sterling mine area have high arsenic, antimony, mercury and thallium contents (Odt, 1983; Hill et al., 1986). Tingley (1984) reported high arsenic, antimony and molybdenum contents in samples from the Telluride, Sterling, and Daisy mine areas, and high lead and zinc from the latter two areas.

The presence of hydrothermal alteration, fluorite, and locally elevated gold concentrations in porphyry dikes indicates that much, or all, of the mineralization in Bare Mountain postdates emplacement of the dikes. K/Ar and Ar/Ar ages of about 12.9 Ma have been obtained on hydrothermal potassium feldspar that replaces groundmass and phenocrysts of igneous potassium feldspar in altered dike rock at the Goldspar mine, indicating that hydrothermal activity took place there during the

main magmatic stage of the SWNVF (Noble et al., 1991). Close similarities in mineralization style and trace-element signatures support a similar timing for gold mineralization in pre-Cenozoic rocks in the vicinity of the Daisy mine. At the nearby Secret Pass deposit, hydrothermal alteration extends into the ca. 13-Ma Topopah Spring Member of the Paintbrush Tuff, but not into adjacent exposures of the 11.6-Ma Rainier Mesa Member of the Timber Mountain Tuff. In the Telluride mine area, alunite occurs in altered gravel in the hanging wall of the Fluorspar Canyon fault and in hydrothermal breccia in the footwall of the fault. Samples of this alunite were dated at 12.2 ± 0.4 Ma and 11.2 ± 0.3 Ma, respectively, by K/Ar methods (Jackson, 1988). Alunitic alteration is also found near the Mother Lode mine in bedded tuff between the Paintbrush Tuff and Rainier Mesa Member of the Timber Mountain Tuff.

The dated alunite is fine grained, suggesting either a supergene origin or a vapor-dominated depositional environment (e.g., Thompson, 1991), and the dates, therefore, may represent minimum ages for mineralization. If the alunite was deposited by hypogene fluids, the ages suggest the possibility of more than one period of activity or that hydrothermal activity in the Telluride–Mother Lode area was of long duration.

A number of lines of evidence suggest a shallow or high-level environment for mineralization in Bare Mountain. Hydrothermal breccia in the Sterling, Goldspar and Telluride mine areas is suggestive of a high-level environment. The altered Tertiary volcanic rocks present in fluoritized breccia at the Goldspar mine include clasts of the Paintbrush Tuff. The most reasonable interpretation is that the volcanic rock fragments fell into the breccia prior to, or during, hydrothermal activity. Because the age of hydrothermal activity is essentially the same as the age of the Paintbrush Tuff, the deposit was probably open to the paleosurface. Cinnabar and high mercury concentrations are widespread in northern and eastern Bare Mountain and alunite ± opal is present in several mineralized areas. Such mineral associations are considered indicative of a shallow hydrothermal environment, although it is possible that the alunite is not entirely hypogene.

Noble et al. (1989) inferred the presence of a buried, granite-type porphyry molybdenum system in Bare Mountain from the presence of porphyry-style crystallization textures and hypersaline fluid inclusions in the felsic dikes, the spatial association of mineralization with the dikes, and the fluorite-molybdenum component of the trace-element assemblage of the mineralization in Bare Mountain. Gold-silver-mercury-fluorite mineralization in Bare Mountain may represent the distal, near-surface expression of hydrothermal activity related to a deeper porphyry molybdenum system (Noble et al., 1989).

Mine Mountain

Mine Mountain, in the southeast part of the SWNVF (Fig. 1), was the site of mercury, base-metal, and precious-metal prospecting in the 1920s, but was subsequently included in the Nevada Test Site and withdrawn from mineral entry. A 2-km-long northeast-trending area along the crest of Mine Mountain contains quartz ± calcite ± barite ± sulfides in veins, hydrothermal breccia, and silicified areas (Quade et al., 1984; L.T. Larson and S.I. Weiss, unpubl. mapping, 1989). Mineralization is closely associated with the flat-lying Mine Mountain thrust fault, which separates underlying Mississippian clastic rocks from Devonian carbonate rocks in the upper plate (Orkild, 1968). The mineralization occurs both above and below the thrust fault, but appears to be most strongly developed within a few tens of meters above the fault in highly brecciated rock (L.T. Larson and S.I. Weiss, unpubl. mapping, 1989).

Above the Mine Mountain thrust, mineralization is closely associated with moderate- to high-angle northeasterly-striking faults and

fractures, and north- to northwest-striking high-angle fractures. Subhorizontal slickensides on these structures indicate lateral slip, probably related to movements along the nearby, northeast-trending, left-slip Mine Mountain fault zone of Carr (1984). Locally, quartz-barite veins both crosscut and are offset by faults with subhorizontal slickensides, indicating that mineralization was coeval with strike-slip movement.

In the lower plate of the Mine Mountain thrust, quartz- and calcite-cemented fault and hydrothermal breccia comprise narrow veins that trend NW to nearly E–W and can be traced for as much as 1 km in clastic rocks of the Eleana Formation. Samples of these veins, which yielded the highest gold analyses of any rocks from Mine Mountain, contain very finely granular to chalcedonic quartz along with alunite and cinnabar. SEM/EDX examination of a breccia-vein sample with 0.6 ppm gold and very high arsenic and lead contents shows an arsenate, iodide and selenide assemblage including mimetite ($3Pb_3(AsO_4)_2 \cdot PbCl_2$), conichalcite ($8(Cu,Ca)As_2O_3 \cdot 3H_2O$), tocornalite (HgAgI), and tiemannite (HgSe). Trace amounts of pyrite and arsenopyrite are also present.

Alteration mineralogy at Mine Mountain is dominated by fine-grained silicification. In massive carbonate rocks in the upper plate, silicification includes variable amounts of chalcedonic replacement (jasperoid) and millimeter- to centimeter-wide sheeted or stockwork quartz veins. White calcite veins are abundant in carbonate rocks surrounding the area of silicification. Vein quartz has fine- to medium-granular or fine comb textures, and clear drusy quartz is also present. Barite, calcite, galena, sphalerite and anglesite have been identified in veins and silicified rocks. Cinnabar is present in veins and is also disseminated in leached, decalcified and silicified carbonate rocks. Small amounts of gossan are associated with massive white calcite and barite-rich hydrothermal breccia.

Samples from Mine Mountain have high base-metal contents, along with an epithermal precious-metal suite that includes arsenic, antimony and mercury (Table 2). Lead, zinc, selenium, cadmium, antimony and mercury contents are very high relative to other mineralized areas in the SWNVF. The gold and silver correlation with base metals is strong at Mine Mountain (Fig. 3). The correlation between gold and selenium is particularly striking, but silver correlates much more strongly with cadmium, mercury and base metals than does gold. The gold–silver correlation is weaker at Mine Mountain than it is in other mineralized areas in the SWNVF (Fig. 3).

The timing of hydrothermal activity at Mine Mountain is constrained by indirect stratigraphic and structural relations. Based on the presence of argillic and alunitic alteration in tuffs as young as the Ammonia Tanks Member of the Timber Mountain Tuff on the south flank of Mine Mountain, Jackson (1988) inferred the mineralization to be approximately contemporaneous with Timber Mountain magmatic activity. Alunite from an outcrop of the altered Ammonia Tanks Member has given a K/Ar age of 11.1 ± 0.3 Ma (E.H. McKee, S.I. Weiss and L.T. Larson, unpubl. data, 1989), consistent with alteration shortly after deposition of the 11.4-Ma Ammonia Tanks Member. Alteration has not been traced from the dated outcrop directly into the main mineralized area. However, if syn-mineralization lateral slip movements on fault surfaces along the crest of Mine Mountain were associated with deformation along the Mine Mountain strike-slip fault system, which offsets both units of the Timber Mountain Tuff (Orkild, 1968; Carr, 1984), then mineralization occurred after 11.4 Ma as well, consistent with the K/Ar age of the alunitic alteration.

The geochemical data at Mine Mountain are consistent with mineralization from more than one hydrothermal system. Base-metal and silver vein or replacement mineralization in Paleozoic sedimentary rocks may have been re-

mobilized and overprinted by later epithermal metallization during magmatic activity of the Timber Mountain stage of the SWNVF.

Bullfrog district

The Bullfrog district in the Bullfrog Hills west of the town of Beatty (Fig. 1) has been the most important source of precious metals in the SWNVF. The district contains gold-silver vein deposits that are scattered within large areas underlain by hydrothermally altered rock, particularly in the southern part of the Bullfrog Hills (Fig. 2).

The Original Bullfrog mine in the southwest corner of the Bullfrog district was discovered in 1904, but most early production came from the Montgomery–Shoshone mine 6.5 km to the east (Fig. 2). By 1940, the Bullfrog district had recorded precious-metals production totalling about $3 million (Couch and Carpenter, 1943). Minor precious-metal production came from the Gold Bar mine and from several mines near the town of Rhyolite. The Mayflower and Pioneer mines, about 12 km north of Rhyolite, also had minor early production. Renewed exploration in the district since the mid-1970s resulted in open-pit mining for three years at the Gold Bar mine, the delineation of open-pit mineable reserves at the Montgomery–Shoshone mine, and the discovery and development of the Lac Bullfrog mine (Fig. 2), an entirely new deposit on the east side of Ladd Mountain that is expected to produce at least 61 t (1.8 million oz) of gold.

The Bullfrog Hills consist of an imbricately normal-faulted allochthon, composed mostly of Miocene volcanic and sedimentary rocks, that is separated from underlying Paleozoic and Proterozoic sedimentary and metamorphic rocks by a low-angle fault first recognized by Ransome et al. (1910). This structure is the Original Bullfrog segment of the regional OB–FC detachment fault system (Fig. 2) (Carr and Monsen, 1988; Maldonado, 1990a). Upper-plate rocks consist chiefly of silicic ash-flow sheets including units of the Crater Flat, Paintbrush and Timber Mountain Tuffs that were erupted from the central caldera complex of the SWNVF between about 15 and 11.4 Ma (Table 1). Lesser volumes of lava flows, domes and local tuffs of silicic composition, and relatively minor amounts of mafic and intermediate composition lava flows are intercalated with the regional ash-flow sheets. Units of tuffaceous sandstone, conglomerate, shale and lacustrine limestone are present mainly in the lower part of the volcanic section. Lying with angular discordance upon the Timber Mountain Tuff and older ash-flow sheets, is a local sequence of interbedded rhyolitic flows, domes and associated pyroclastic deposits which are capped by latite flows. These post-Timber Mountain Tuff rocks were erupted prior to about 10 Ma (Marvin et al., 1989; Noble et al., 1991).

Throughout much of the Bullfrog Hills, upper-plate rocks are cut by numerous west-dipping normal faults, many of listric geometry, that mostly strike north to northeast. This deformation has long been recognized as the result of WNW–ESE-directed upper crustal extension, and estimates of the amount of extension range from about 25% (Ransome et al., 1910) to more than 100% (Maldonado, 1990a). Most of the faulting and tilting began after about 11.4 Ma, as demonstrated by conformable and paraconformable relations between the Ammonia Tanks Member of the Timber Mountain Tuff and underlying ash-flow sheets in the southern Bullfrog Hills. Major tilting and faulting ceased before deposition of the flat-lying, 7.6-Ma Spearhead Member of the Stonewall Flat Tuff and local late Miocene conglomeratic deposits (Weiss et al., 1990).

Original Bullfrog mine

The Original Bullfrog mine was developed in a complex, shallowly north-dipping vein that is approximately 10 m thick. The vein is a shattered mass of banded crustiform quartz,

calcite and silicified breccia that lies along the Original Bullfrog fault (Ransome et al., 1910). This fault, which appears to truncate the vein material against underlying, strongly sheared Paleozoic clastic and carbonate rocks that contain only minor veining, is part of the Bullfrog detachment fault system of Maldonado (1990a, b). The main vein grades upwards into sheeted veins within moderately east-dipping silicified ash-flow tuff of the 13.85-Ma Lithic Ridge Tuff (Carr et al., 1986; Sawyer et al., 1990). Adularia and albite replace feldspar phenocrysts and groundmass potash-feldspar and locally, between closely spaced veins, the tuff has been pervasively adularized. This alteration grades laterally and up-section into quartz-illite and sericite-albite-calcite assemblages, and at greater distances, into weak illite-calcite ± albite alteration.

Vein quartz ranges from white, yellow and grey, banded fine granular or chalcedonic material to white, clear or amethystine, fine to medium comb quartz. Calcite occurs as coarsely crystalline masses intergrown with comb quartz, as inwardly-growing crystals along the walls of veins that were subsequently filled with comb quartz, or as irregular drusy veins with little or no quartz.

In addition to quartz and calcite, the main vein carries visible gold that is associated with limonite, malachite, chrysocolla and sulfide. SEM/EDX examinations of high-grade ore show that gold occurs in irregular electrum grains up to 1 mm in diameter with compositions that range between $Au_{52}Ag_{48}$ and $Au_{42}Ag_{58}$. Gold also occurs in mixed grains of native metal ($Au_{80}Ag_{20}$) and uytenbogaardtite (Ag_3AuS_2) (Fig. 6A). Silver is also present as acanthite, which occurs as irregular grains in quartz, and as mixed grains with uytenbogaardtite and gold. Textural relations indicate a complex paragenetic sequence. In ore containing visible gold, early calcite was followed by white comb quartz with sulfide and electrum, and lastly by vein-filling grey to amethystine quartz. The calcite is locally replaced by malachite and chrysocolla, which also occur in irregular masses surrounding gold and sulfide, and in late veinlets with sulfide and limonite. Textural relationships indicate that electrum is the earliest ore mineral, followed by acanthite, uytenbogaardtite and gold.

Samples from the Original Bullfrog mine have relatively high average silver:gold when compared to other mineralized areas in the Bullfrog district (Table 2). In addition, Original Bullfrog samples have strong copper, antimony and bismuth correlations with gold (Figs. 3 and 5).

Adularia from altered Lithic Ridge Tuff adjacent to the main vein has a K/Ar age of 8.7 ± 0.3 Ma (Jackson, 1988) indicating that hydrothermal activity took place about 1–1.5 million years after the end of volcanic activity in the Bullfrog Hills. This age, along with shattering of the vein and apparent truncation of the vein by the underlying Original Bullfrog fault, is consistent with mineralization during the major period of detachment-style faulting in the region between 11.4 and 7.6 Ma.

Gold Bar mine

At the Gold Bar mine in the northwest corner of the Bullfrog district (Fig. 2), silver-gold mineralization is present in quartz-calcite veins and quartz-calcite-cemented breccia along a northeast-trending, west-dipping normal fault system cutting units of the Crater Flat and Paintbrush Tuff and minor basaltic rocks. The main area of mineralization lies about 2 km from the surface trace of the Bullfrog detachment fault system (Maldonado, 1990a). Veins consist of banded crustiform intergrowths of calcite and fine granular and comb quartz, commonly with drusy quartz and calcite and minor amethystine comb quartz. Late calcite veins are also present. Pyrite is the only sulfide mineral reported in vein material at the Gold Bar mine (Ransome et al., 1910). Wall-rock alteration appears to be similar to that at the Original Bullfrog mine. Variable albitization and adularization of feldspar phenocrysts and

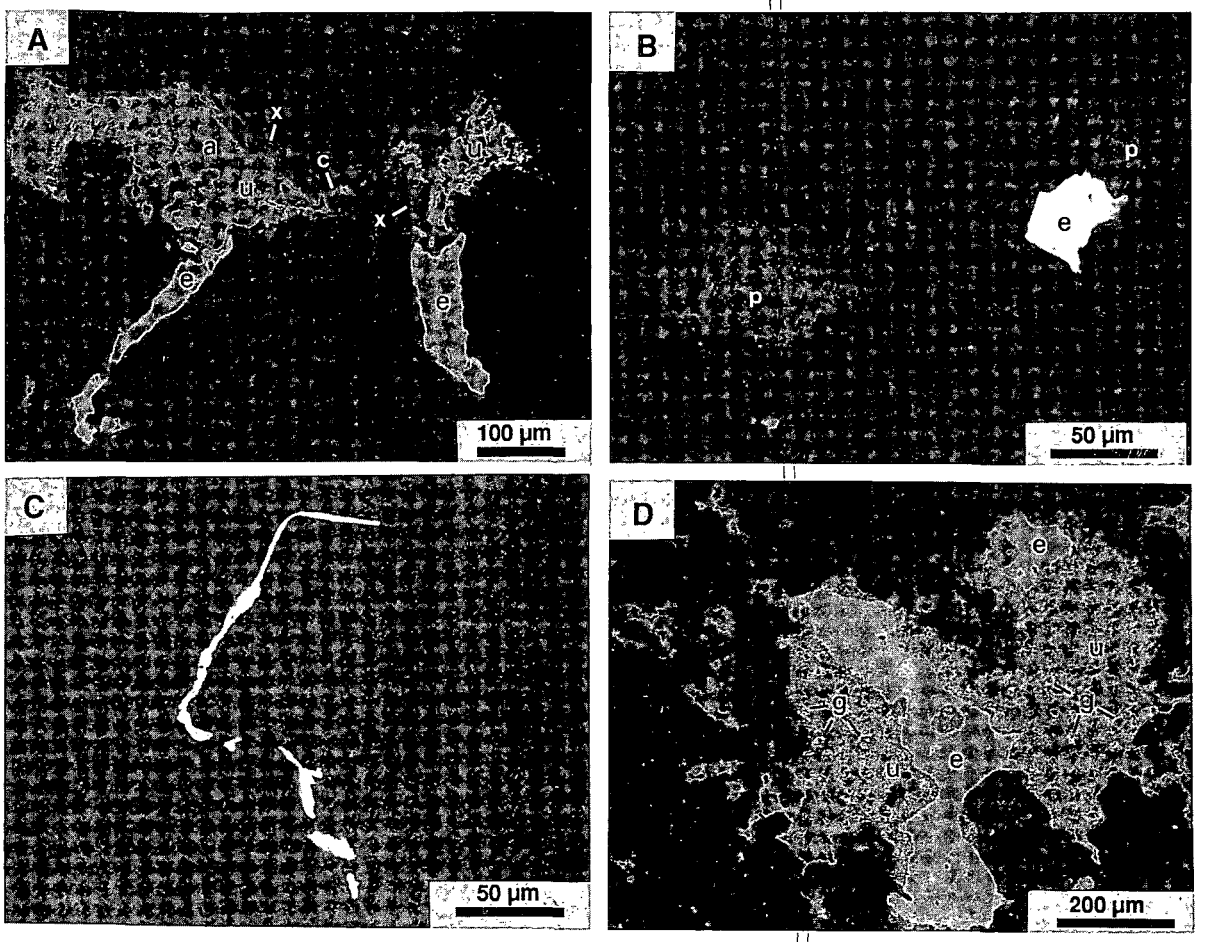

Fig. 6. Backscattered SEM photomicrographs of electrum in ore from the Bullfrog district. (A) Electrum (*e*) with associated Sb–Bi–Cu phase (×) and inner zones of chrysocolla (*c*), acanthite (*a*), and uytenbogaardtite (*u*) in vein from the Original Bullfrog mine. (B) Electrum (*e*) replacing limonitized pyrite (*p*) in Lac Bullfrog ore. (C) An irregular flake of electrum in Lac Bullfrog ore. (D) Electrum (*e*) partially replaced by uytenbogaardtite (*u*) that contains gold-rich electrum grains (*g*) in Lac Bullfrog ore.

groundmass, along with illite/sericite alteration, are associated with silicification adjacent to veins. Disseminated pyrite is also present in unoxidized altered wall rock.

Samples collected from the Gold Bar mine have a moderate average silver:gold ratio and show only a weak gold-copper association (Figs. 3 and 5). Arsenic, antimony, mercury and the base metals are extremely low (Table 2). The highest gold and silver contents are in veins of finely crystalline quartz with intergrown thinly bladed calcite (Fig. 7A).

Alteration and mineralization at the Gold Bar mine postdate deposition of the ca. 13- to 12.7-Ma Paintbrush Tuff but have not been dated directly. Vein and alteration styles, textures, and mineral assemblages are similar to those of other deposits in the Bullfrog district, suggesting that mineralization at the Gold Bar mine is genetically related to mineralization elsewhere in the district. In addition, veins at the Gold Bar mine were localized by upper-plate faults that were probably active during detachment-related extensional deformation between 11.4 and 7.6 Ma, indicating vein emplacement at approximately the same time as

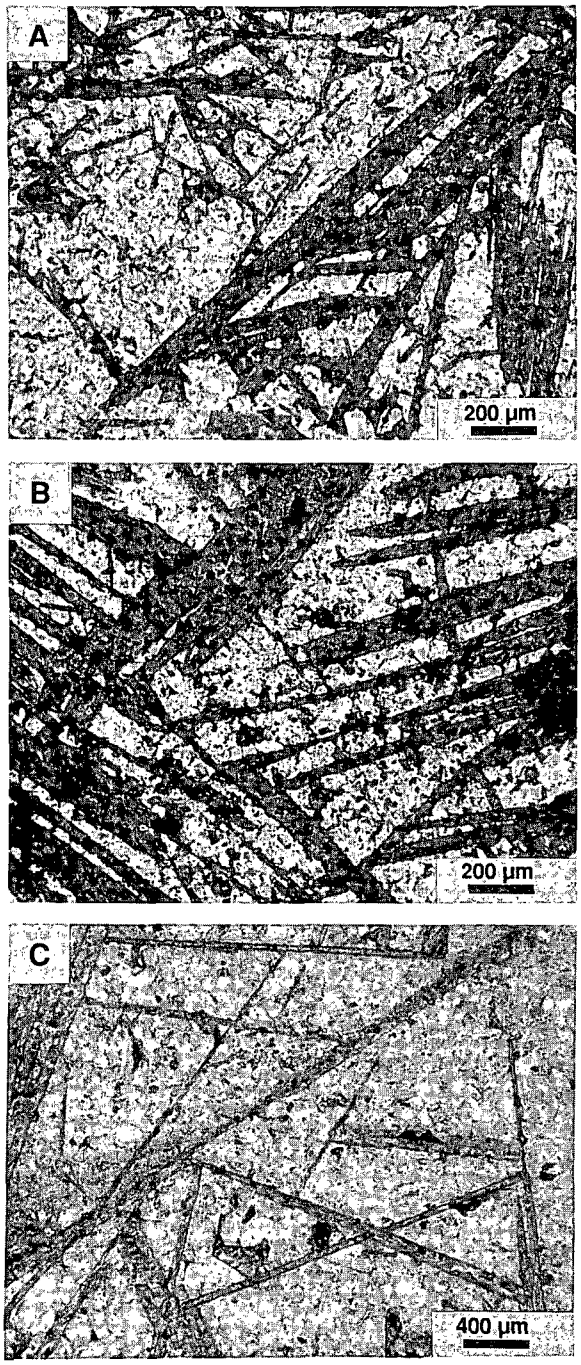

Fig. 7. Finely bladed calcite (dark) in quartz from (A) Gold Bar, (B) Lac-Bullfrog, and (C) Mayflower mines. Photomicrographs A and B, reflected light; photomicrograph C, transmitted light.

mineralization in the other deposits (see below).

Rhyolite area

The Rhyolite area contains the largest and highest grade known gold-silver ore reserves in the SWNVF. It includes vein systems at the Montgomery–Shoshone mine, the Lac Bullfrog mine and several small mines near the town of Rhyolite (Fig. 2). Most of the reserves are in the Lac Bullfrog deposit where Jorgensen et al. (1989) reported 13.0 Mt of ore averaging 3.77 g/t (14.3 Mst at 0.110 oz/st) prior to the start of production. By the end of 1991, 16.4 t (480,000 oz) of gold had been produced from this deposit, and reserves were estimated at 48 t (1.4 million oz) of economically mineable gold (D. McClure, pers. commun., 1991). Most of the historic gold and silver production in the Bullfrog district came from the Montgomery–Shoshone mine, about 1.5 km northeast of Rhyolite (Couch and Carpenter, 1943), which has reserves of 2.8 Mt of gold ore at an average grade of 2.5 g/t (3.1 Mst at 0.072 oz/st) as reported by Jorgensen et al. (1989). Host rocks for veins in the Rhyolite area are predominantly densely welded, devitrified portions of ash-flow sheets of the Paintbrush and Timber Mountain Tuffs.

At the Lac Bullfrog mine gold-silver ore is mined from a moderately west-dipping vein system that lies along a normal fault ("middle-plate fault" of Jorgensen et al., 1989) at the eastern foot of Ladd Mountain. Ore comprises a central zone, as much as 70 m thick, of complexly cross-cutting veins, hydrothermal breccia and silicified volcanic rock, that lies within the vein system. Closely spaced veins in the ore zone form stockworks and sheeted vein swarms. More widely spaced veins also form stockworks above and below the ore zone (Jorgensen et al., 1989). Well developed faults that have been the locus of significant displacement bound the ore zone in most places and are accompanied by gold-rich hydrothermal breccia (B. Claybourn, pers. commun.,

1991). The hanging-wall rocks are well exposed on Ladd Mountain, an east-tilted fault-block that is composed mainly of a pervasively altered section of the Timber Mountain Tuff, a thin basaltic flow or sill, and underlying units of the Paintbrush Tuff and Crater Flat Tuff (Maldonado and Hausback, 1990). Exposed footwall rocks include strongly altered rocks probably belonging to the Crater Flat Tuff and an underlying unit of dacitic to rhyodacitic lava that is widely exposed beneath the Crater Flat and Lithic Ridge Tuffs elsewhere in the Bullfrog Hills (c.f., Maldonado and Hausback, 1990).

Vein material consists mostly of crustiform fine granular and comb quartz (locally amethystine) ± intergrown calcite of anhedral to finely bladed habit (Fig. 7B). Bands and veins of very finely granular to chalcedonic quartz and moderately coarse comb quartz are also present, and bands of fine adularia occur in minor amounts. Fluorite and barite have also been reported (Jorgensen et al., 1989). Fragments of wall rock are included in the veins and have been partly to nearly completely replaced by fine-grained quartz and adularia.

Multiple generations of cross-cutting quartz ± calcite veins, open space infillings, and fragments of vein material surrounded by later stages of quartz ± calcite provide evidence for a multi-stage paragenesis and for fracturing and brecciation concurrent with vein deposition. Much of the vein material is highly fractured, and faults generally form the margins of the main ore zone. These features suggest that the latest movements on the host fault postdate the last stages of vein deposition.

The style of mineralization at the Montgomery–Shoshone mine is similar to that at the Lac Bullfrog deposit (Jorgensen et al., 1989). Most of the gold-silver ore came from veins and breccia along a major, northeast-trending high-angle fault that juxtaposes unmineralized and unaltered, to very weakly altered, post-Timber Mountain rhyolitic to latitic rocks on the north against strongly altered rocks, mainly of the Ammonia Tanks Member of the Timber Mountain Tuff, to the south.

Mineralization extends southward for as much as 0.5 km in and along several north-trending quartz-calcite veins that occupy fractures and minor faults (Jorgensen et al., 1989; Maldonado and Hausback, 1990). Faults and fractures that control mineralization are part of the imbricate fault system associated with extension above the OB–FC fault (Maldonado, 1990a).

A number of smaller gold-silver bearing quartz and quartz-calcite veins similar to those of the Lac Bullfrog and Montgomery–Shoshone deposits were mined in the immediate vicinity of Rhyolite. The most notable workings include those of the National Bank mine, where sheeted and stockwork veins of fine granular quartz cut silicified and adularized tuffs of the Paintbrush Tuff and the Rainier Mesa Member of the Timber Mountain Tuff. At the Denver–Tramp mine these units host a system of subparallel steeply dipping north–south-trending quartz-carbonate veins up to 8 m wide that carry visible gold. The Denver–Tramp veins contain banded, very finely granular to fine comb quartz that is locally amethystine, and pockets of calcite that has been partially leached, leaving dark earthy manganese and iron oxides.

In addition to local silicification, mineralization in the Rhyolite area is associated with locally pervasive adularia flooding and more widespread adularia and albite replacement of feldspar phenocrysts. Thin veins within the Rainier Mesa Member on Ladd Mountain west of the Lac Bullfrog mine have adularized envelopes up to 1 cm thick, and sheeted veins at the National Bank mine occur in hard rock composed almost completely of adularia. In the Lac Bullfrog, Montgomery–Shoshone, National Bank, and Denver–Tramp mines, near-vein alteration consists of replacement of feldspar phenocrysts with adularia ± albite (Fig. 8) and probable adularization of groundmass feldspar. Small amounts of illite are present,

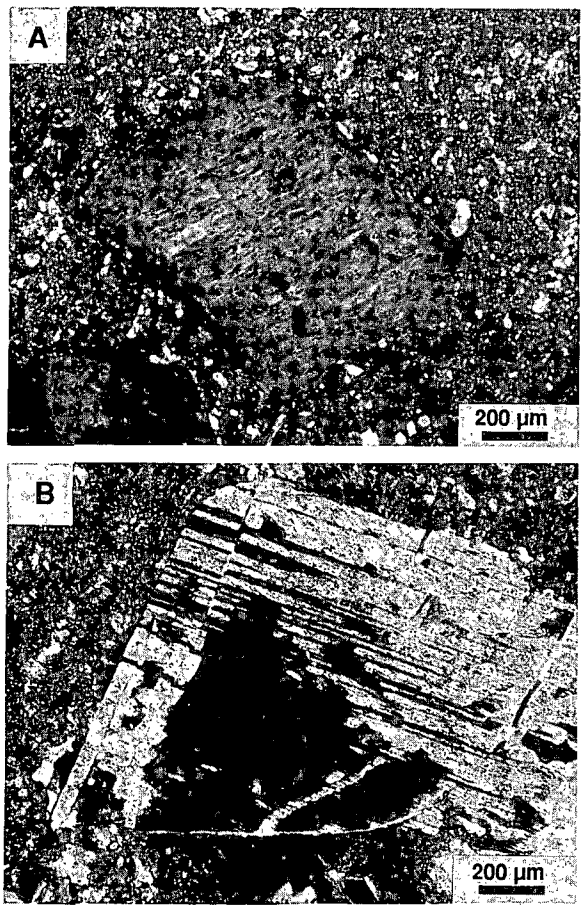

Fig. 8. Photomicrographs in cross-polarized transmitted light of (A) adularized, and (B) albitized feldspar phenocrysts in near-vein altered rhyolite tuff from the Lac Bullfrog mine. Identical alteration is present at the Original Bullfrog, Montgomery–Shoshone, Gold Bar, Mayflower, and Pioneer mines.

generally intergrown with secondary K-feldspar and quartz. Strong phyllosilicate alteration is uncommon in the Rhyolite area, except locally at the Montgomery–Shoshone mine. Primary biotite is commonly preserved, even in strongly altered rocks, reflecting the high activity of K^+ needed to produce adularia. At the Bold Gold Bullfrog mine pseudomorphs of limonite after pyrite are present in oxidized rock, and unoxidized rocks contain 1–2% disseminated pyrite.

Near-vein alteration described above grades outward from mineralized structures to much more subtle, but nevertheless pervasive and widespread illite-calcite ± quartz ± albite assemblages that could be considered propylitic in character (e.g., Sander and Einaudi, 1990). Chlorite- and carbonate-bearing assemblages have been reported only from sedimentary and metamorphic rocks beneath the Original Bullfrog–Fluorspar Canyon fault (Jorgensen et al., 1989).

All of the gold identified visually in samples from the Rhyolite area was found in fine granular and comb quartz. Very fine granular vein quartz is generally present in gold ore, but was not seen to contain gold. Finely bladed calcite intergrown with quartz in vein material from the Lac Bullfrog mine is similar to that observed in vein material from the Gold Bar mine. Acanthite is a major silver-bearing phase in some ore at the Lac Bullfrog mine and minor amounts of chalcopyrite, galena and sphalerite have also been reported (Jorgenson et al., 1989). Cerargyrite was reported at the Montgomery–Shoshone mine by Ransome et al. (1910). Secondary copper minerals are locally associated with gold at depth in the Lac-Bullfrog mine (B.W. Claybourn, pers. commun., 1991) and tetrahedrite has also been identified (D. Brosnahan, pers. commun., 1991). This mineral association is similar to that at the Original Bullfrog mine.

Ransome et al. (1910) reported that gold in the Bullfrog district characteristically occurs as electrum in limonitic specks that represent oxidized pyrite crystals. Electrum of this type is present at the Lac Bullfrog mine as well (Fig. 6B). We found other types of gold in the district. Electrum occurs as contorted flakes between quartz grains (Fig. 6C) at the Lac Bullfrog and Denver–Tramp mines. SEM/EDX analysis shows that electrum in this form from the Lac Bullfrog mine has a composition of $Au_{44}Ag_{56}$. In addition, electrum and gold are present in irregular lenses composed of quartz, limonite, chrysocolla, acanthite and uytenbogaardtite, that are similar to mineralization described above at the Original Bullfrog mine.

The electrum ($Au_{57}Ag_{43}$ to $Au_{51}Ag_{49}$) is in irregular grains up to 1 mm in maximum dimension, and gold ($Au_{72}Ag_{28}$) is present as narrow borders on electrum. The uytenbogaardtite is intergrown with gold ($Au_{72}Ag_{28}$ to $Au_{77}Ag_{23}$) and acanthite, and appears to replace electrum (Fig. 6D).

Most samples of veins and altered volcanic rocks from the Rhyolite area contain elevated gold and silver contents relative to unaltered silicic volcanic rocks, but have low contents of other trace elements (Table 2). A sample of unusually rich ore containing 9223 ppm gold and 2.1% silver from the Lac Bullfrog mine is an exception, containing high copper, lead, antimony, zinc, selenium and tellurium. A few samples contain anomalous molybdenum or tellurium, but copper is the only trace element that correlates well with precious metals (Fig. 3). Copper reportedly increases in abundance with depth at the Lac Bullfrog mine (Jorgenson et al., 1989) Arsenic is remarkably low; maximum arsenic content in samples that we obtained from the Rhyolite area is 88 ppm, and arsenic values are not correlative with gold (Figs. 3 and 5).

Alteration and mineralization in the Rhyolite area postdate deposition of the 11.4-Ma Ammonia Tanks Member of the Timber Mountain Tuff and are structurally controlled by faults and fractures that formed in the upper plate of the Bullfrog detachment system during the period of regional extensional faulting between 11.4 and 7.6 Ma. A K/Ar age of 9.5 ± 0.2 Ma on adularia from the Montgomery–Shoshone mine (Morton et al., 1977) indicates that mineralization took place there during this period. Fault relationships and quartz-healed brecciation in the Lac Bullfrog vein are consistent with mineralization that took place during faulting and prior to the last movements along the controlling structure. The similarities in structural control, mineralogy, style of veins, and alteration lead us to infer that mineralization throughout the Rhyolite area took place at about the same time as that at the Montgomery–Shoshone mine.

Mayflower–Pioneer area

The Mayflower and Pioneer mines, about 12 km north of Rhyolite, were developed between 1905 and the early 1920s, but little production was recorded (Ransome et al., 1910; Cornwall, 1972). The original gold strike at the Pioneer mine consisted of mineralized gouge and breccia along a steeply southwest-dipping shear zone (unpubl. inf., NBMG mining district files). At the Mayflower mine, gold ore was found in a southwest-dipping fracture zone with sheeted to irregular quartz-calcite veins (Ransome et al., 1910). Both mines are in rocks containing adularia-albite-illite alteration and quartz-calcite veining similar to that in the Rhyolite area. Host rocks include the Crater Flat Tuff as well as overlying coarse volcaniclastic and megabreccia deposits consisting of debris that includes pre-Tertiary rock and ash-flow units as young as the 11.4-Ma Tuffs of Fleur de Lis Ranch (S. Weiss and K. Connors, unpubl. mapping, 1990). The coarse clastic rocks are overlain by rhyolitic tuffs and lavas erupted by about 10 Ma (Marvin et al., 1989; Noble et al., 1991).

Analyses of a small number of mineralized and altered samples reported gold values as high as 15.3 ppm along with high mercury and antimony, but relatively low arsenic. A vein sample from the Mayflower mine was found to contain fine grey comb quartz with finely bladed calcite (Fig. 7C) similar to that found in gold-rich veins in the Rhyolite area and at the Gold Bar mine. Veins in the Mayflower mine contain electrum in limonite and as contorted flakes similar to occurrences in the Rhyolite area (c.f., Figs. 6B and C).

Adularia from mineralized rock at the Mayflower mine has a K/Ar age of 10.0 ± 0.3 Ma (Jackson, 1988), consistent with stratigraphic constraints. This date overlaps, within analytical uncertainty, the adularia age-date for the Montgomery–Shoshone mine, but is appreci-

ably older than the date reported for adularia from the Original Bullfrog mine.

Discussion

Hydrothermal activity and precious-metal mineralization in the southern part of the SWNVF took place over a period of approximately 4.5 million years that overlapped with episodes of magmatic activity. Although all of the mineralization is epithermal in nature, its style and geochemistry vary significantly from area to area (Table 4).

Silver-gold mineralization in the Wahmonie district differs from mineralization in other parts of the SWNVF in that it is situated in the eroded remnants of a volcanic center dominated by rocks of intermediate composition. K/Ar ages indicate that hydrothermal activity at Wahmonie occurred during the main magmatic stage of the SWNVF, and coincided with, or closely followed, the end of magmatic and volcanic activity at the Wahmonie–Salyer volcanic center. Based on mineral assemblages in ore, vein, and wall rock alteration, type of host rocks, and available geochemical data, mineralization at Wahmonie comprises an epithermal precious-metal system of the adularia-sericite type of Heald et al. (1987) or the low sulfur type of Bonham (1989).

Available data show that base metals, arsenic, antimony and mercury at Wahmonie are relatively low compared to high base-metal, adularia-sericite type deposits (e.g., Creede, Colorado, Heald et al., 1987), and suggest kinship with high silver:gold ratio, relatively base-metal-poor deposits such as Tonopah, Nevada (e.g., Bonham, 1989). However, the high bismuth and tellurium concentrations of the Wahmonie district are not typical of adularia-sericite type precious-metal deposits; these elements are more commonly associated with

TABLE 4

Summary of precious-metal mineralized areas in the southern part of the southwestern Nevada volcanic field

District	Host Rocks	Mineralization		Trace Element Assemblage	Structural Setting
		Style	Age (Ma)		
Wahmonie	andesitic to rhyodacitic volcanic and intrusive rocks ca. 13 Ma	adularia-sericite type; quartz-calcite veins, sheeted veins	13-12.5	Ag+Au+Te+Bi+Hg ±Sb; moderate to high Ag:Au	normal faults
Bare Mountain (Sterling, Daisy, and Mother Lode mines; Secret Pass, Goldspar, and Telluride deposits)	Precambrian + Paleozoic clastic and carbonate sedimentary rocks; felsic intrusives and tuffs ca. 13-11.4 Ma	mostly disseminated; minor quartz-adularia veinlets; fluorite veins	13-11.2(?)	Au+Ag+Sb+As+F ±Hg±Te±Tl±Mo ±Cu±Pb; low Ag:Au	thrust fault; low- to high angle normal faults in part associated with detachment
Mine Mountain	Devonian carbonate rocks and Mississippian clastic rocks	veins, hydrothermal breccia, jasperoid	<11.4	Ag+Au+Pb+Zn+Sb +As+Hg+Cd±Se; very high Ag:Au	thrust fault; high-angle normal and strike-slip faults
Bullfrog (Original Bullfrog, Gold Bar, Mayflower, and Pioneers mines; Rhyolite area: Lac Bullfrog and Montgomery-Shoshone mines)	mainly rhyolitic ash-flow tuff units ca. 14-11 Ma	adularia-sericite type; quartz-calcite veins, sheeted veins and stockworks	9-10	Au+Ag±Cu±Sb; other trace elements generally low; low to moderate Ag:Au	low- to high-angle normal faults associated with detachment

porphyry-related gold deposits such as the Top deposit at Bald Mountain and the Fortitude and McCoy deposits in Nevada (e.g., Bonham, 1989; Brooks et al., 1991). Two other characteristics of the Wahmonie area suggest that exposed and near-surface mineralization may be associated with an underlying porphyry system. First, subvolcanic stocks and rhyolite dikes exposed in the central horst as well as geophysical evidence for a pluton beneath the district are consistent with the presence of a buried, perhaps composite, porphyry intrusion. Secondly, the presence of hypersaline fluid inclusions in quartz phenocrysts and biotite ± tourmaline veins within the porphyritic granodiorite argue strongly for at least some porphyry-type magmatic-hydrothermal activity.

Precious-metal mineralization in the Bare Mountain district, although apparently similar in age to that at Wahmonie, occupies an entirely different geologic setting. Mineral assemblages, chemistry, and style of Bare Mountain mineralization and alteration are also markedly different from the Wahmonie district. Stratigraphic, structural and radiometric age relations indicate that gold-silver ± mercury ± fluorite mineralization in Bare Mountain took place during the main magmatic stage of the SWNVF subsequent to the emplacement of the felsic dike swarm. With the exception of the Secret Pass deposit, areas of gold-silver mineralization in northern and eastern Bare Mountain have geochemical and geologic characteristics of Carlin-type, sedimentary rock-hosted disseminated deposits (e.g., Radtke, 1985, Percival et al., 1988). Gold deposits in Bare Mountain consists of disseminated mineralization in sedimentary, hypabyssal, and extrusive rocks with only minor quartz veining, little or no silicification, and common fluorite and cinnabar. Alteration is mainly illitic to kaolinitic with decalcification ± silica replacement of sedimentary rocks. Remobilized carbon is conspicuous at the Mother Lode deposit. High contents of arsenic, antimony, mercury and molybdenum as well as anomalous thallium are associated with mineralization in the north and east parts of Bare Mountain, and base metals are locally high. Silver contents, however, are generally low, and silver:gold ratios are distinctly lower than in other areas of precious-metal mineralization in the southern part of the SWNVF.

The Secret Pass deposit differs from the sediment-hosted deposits in host-rock lithology, alteration assemblage, and in having lower thallium contents. Although veining and silicification are reported to be weakly developed at Secret Pass (Greybeck and Wallace, 1991), the alteration assemblage, perhaps strongly influenced by host lithology, best fits that of the adularia-sericite type of epithermal precious-metal system. Similarities in trace-element signatures between the Secret Pass deposit and other Bare Mountain deposits show that host-rock lithology does not play a major role in controlling trace-element assemblages.

Gold-silver mineralization in Bare Mountain is clearly epithermal in nature, and has features strongly suggestive of a shallow level of emplacement; nevertheless, it is similar in several respects to Carlin-type disseminated deposits. As Noble et al. (1989) proposed, the presence of a buried, granite-type porphyry molybdenum system in Bare Mountain is likely on the basis of geologic, geochemical, and fluid-inclusion data. Following Noble et al., we propose that most of the gold-silver deposits in Bare Mountain provide examples of distal disseminated sediment-hosted deposits genetically related to magmatic-hydrothermal systems (e.g., Sillitoe and Bonham, 1990) such as deposits in the Bau District, Sarawak (Percival et al., 1990), Purisima Concepcion, Peru (Alvarez and Noble, 1988) and Barney's Canyon, Utah (Sillitoe and Bonham, 1990).

Sediment-hosted precious-metal mineralization is also present within the SWNVF at Mine Mountain. Structural relations and the K/Ar age of alunitic alteration at Mine Mountain indicate that hydrothermal activity and miner-

alization were, at least in part, concurrent with magmatic and volcanic activity of the Timber Mountain magmatic stage of the SWNVF as first proposed by Jackson (1988). The hydrothermal breccia veins, cinnabar and chalcedonic quartz at Mine Mountain, along with abundant mercury, arsenic and antimony (Table 2), are indicative of epithermal mineralization. Mine Mountain also possesses characteristics common to Carlin-type disseminated gold deposits, including association with a thrust fault, occurrence in sedimentary rocks that are variably decalcified, veined, silicified (including jasperoid) and cut by hydrothermal breccia, and the presence of barite veins. However, the high lead and zinc contents, low thallium contents, high silver:gold ratio, and abundance of quartz in veins at Mine Mountain are not typical of Carlin-type deposits (e.g., Radtke, 1985).

On the basis of geology and trace-element chemistry, Mine Mountain is similar to the Candelaria silver district approximately 150 km northwest of Mine Mountain. At Candelaria, disseminated silver ore is associated with thrust faults and intrusions cutting Mesozoic sedimentary and igneous rocks (Moeller, 1988). Carbonate-quartz veins mined for silver, gold, lead, zinc and antimony are present as well (Page, 1959). Candelaria veins have lead, zinc, arsenic, antimony and cadmium contents similar to the Mine Mountain veins and also carry anomalously high mercury (Hill et al., 1986), though not as high as at Mine Mountain. Alternatively, geochemical and geologic data at Mine Mountain are consistent with more than one period of hydrothermal activity that may, in part, have preceded development of the SWNVF.

A distinctly younger episode of mineralization is present in the Bullfrog district. Hydrothermal activity in the district, at about 9 to 11 Ma, occurred during the latter part of the Timber Mountain magmatic stage and may have extended into the late magmatic stage of the SWNVF as proposed by Jackson (1988). The age of mineralization in the Bullfrog district overlaps with a period of intense extensional tectonism in the Bullfrog Hills that provided structural preparation for mineralization, and may also have displaced mineralized rock.

Vein and alteration mineral assemblages, along with mineralization style, show that mineralization in the Bullfrog district was the result of adularia-sericite (low sulfur)-type hydrothermal activity. Wall-rock alteration in the Bullfrog district, which includes large volumes of rock with subtle adularia and albite replacement of feldspar phenocrysts, is similar to alteration described at Round Mountain, Nevada (e.g., Sander and Einaudi, 1990). Precious-metal mineralization in the Bullfrog district is mainly restricted to several quartz-carbonate vein deposits that are similar to each other in texture and mineralogy (Figs. 6 and 7).

The low content of precious-metal-related trace elements serves to distinguish the Rhyolite area from other areas that contain economic gold and silver mineralization in adularia-sericite systems. In comparison with such systems elsewhere in the Great Basin (e.g., Round Mountain, Tingley and Berger, 1985; Sleeper, Nash et al., 1990; Hollister, Bartlett et al., 1991; Rawhide, Black et al., 1991; and Hart Mountain, Capps and Moore, 1991), altered and mineralized rock from the Rhyolite area has the lowest overall contents of precious-metal pathfinder elements, particularly arsenic, antimony and mercury. Most, but not all, of the samples collected during this study came from the oxidized zone, and low metal contents might be the result of supergene leaching; however, most of the data from the other systems listed above are also from analyses of oxidized material. Rhyolite area mineralization took place in an areally extensive hydrothermal system from which typical epithermal and base-metal elements may have been flushed by late-stage fluids. The uytenbogaardtite that appears to replace electrum in the Lac Bullfrog mine (Fig. 6d) in association with acanthite

may be evidence of such a process, because uytenbogaardtite can only occur in equilibrium with acanthite at temperatures below 113°C (Barton et al., 1978). Alternatively, Rhyolite area mineralization may simply have been introduced by fluids with lower base-metal and pathfinder element budgets than those responsible for other volcanic-hosted precious-metal deposits.

The Gold Bar mine in the northwest part of the Bullfrog district has a similar lack of trace elements to mineralized rock at Rhyolite. In comparison, available trace-element data show that the Original Bullfrog and Mayflower mines have higher trace-element contents. The style of veining and occurrence of uytenbogaardtite in both the Original Bullfrog and Lac Bullfrog deposits (Fig. 6) indicates that physical conditions were similar during precious-metal mineralization in widely separated parts of the Bullfrog district, despite differences in trace-element geochemistry.

Precious-metal deposits in the Gold Bar mine, Original Bullfrog mine, Rhyolite area, Daisy mine–Secret Pass area, and Mother Lode mine are located within 2 km of the trace of the OB–FC detachment fault (Fig. 2). Jorgensen et al. (1989) implied that deposits in the Bullfrog district and Fluorspar Canyon resulted from the same hydrothermal system. We believe that this is not the case. Mineralized rock in the Bare Mountain district contains a consistent suite of trace elements that contrasts with the trace-element suite in the Bullfrog district (with the possible exception of the Mayflower–Pioneer area), and the age of hydrothermal activity in the Bullfrog district is significantly younger than in the Bare Mountain area. Moreover, the quartz-carbonate-adularia veins and style of wall-rock alteration that are typical of the Bullfrog district are uncommon in the Bare Mountain area, and large areas of unaltered rock separate the two districts.

Conclusions

Strong differences in ore and gangue mineralogy, style of mineralization, wall-rock alteration assemblages, and trace-element chemistry between areas of precious-metal mineralization reflect the variable geologic settings and chemical diversity of hydrothermal systems active during the development of the SWNVF. These systems were active over a period of about 4.5 million years that spanned portions of the three magmatic stages of the field and gave rise to a broad spectrum of deposit types. The presence of intrusive porphyry, trace-element suites associated with porphyry-related mineralization, and evidence for the passage of high-salinity fluids suggest that mineralization, during the main magmatic stage of the SWNVF at Bare Mountain and Wahmonie was associated with porphyry-type magmatic systems. At Wahmonie silver-rich vein mineralization of the adularia-sericite type is hosted by an intermediate volcanic center, and is temporally and spatially associated with subvolcanic intrusions. At Bare Mountain, a genetic relationship between porphyry magmatism and shallow Carlin-type gold deposits seems likely.

The relatively base-metal- and silver-rich system at Mine Mountain was apparently active during the Timber Mountain stage of SWNVF volcanism. It shares features with vein and disseminated silver mineralization at Candelaria, Nevada, and may be the result of mineralization from more than one hydrothermal system.

The style of mineralization and alteration in the Bullfrog district is similar to other quartz-adularia precious-metal deposits in the Great Basin. The district contains gold-rich deposits that are largely devoid of epithermal elements and base metals. Hydrothermal activity was coeval with strong extensional tectonism and may have continued into the late magmatic stage of the SWNVF. Mineralization in the Bullfrog district and some deposits in the Bare

Mountain district were structurally controlled by the OB–FC detachment fault system. However, differences in age, mineralization style and geochemistry indicate that mineralization in the two districts is unrelated.

Acknowledgements

Our studies have been partially supported by funds provided by the Nevada Nuclear Waste Project Office through the Center for Neotectonic Studies (to Weiss) and by the U.S. Department of Energy and Science Applications International Corporation (to Castor). J.J. Sjoberg, U.S. Bureau of Mines Western Research Center, Reno, Nevada, is gratefully acknowledged for providing SEM/EDX analyses. We thank M.O. Desilets of the NBMG for calculation of correlation coefficients for the chemical analyses. J.V. Tingley and H.F. Bonham of the NBMG, and L.T. Larson and D.C. Noble of the Mackay School of Mines, University of Nevada, Reno, contributed useful comments and discussion on data and ideas reported herein. J. Quade kindly provided unpublished data on the Wahmonie mining district. We are grateful to the staff of Lac Bullfrog, Inc., GEXA Gold Corp., U.S. Precious Metals, Ltd., and Angst, Inc. for allowing access to their properties, as well as discussions on the geology of their deposits. We thank J.S. Cline and A.B. Wallace for constructive reviews of the manuscript.

References

Alvarez, A.A. and Noble, D.C., 1988. Sedimentary rock-hosted disseminated precious metal mineralization at Purisima Concepcion, Yauricocha district, central Peru. Econ. Geol., 83: 1368–1378.

Bartlett, M.W., Enders, M.S. and Hruska, D.C., 1991. Geology of the Hollister gold deposit, Ivanhoe district, Elko County, Nevada. In: G.L. Raines, R.E. Lisle, R.W. Schafer and W.H. Wilkinson (Editors), Geology and Ore Deposits of the Great Basin, Vol. II. Geol. Soc. Nev., pp. 957–978.

Barton, M.D., Kieft, C., Burke, E.A.J. and Oen, I.S., 1978. Uytenbogaardtite, a new silver-gold sulfide. Can. Mineral., 16: 651–657.

Black, J.E., Mancuso, T.K. and Gant, J.L., 1991. Geology and mineralization at the Rawhide Au–Ag deposit, Mineral County, Nevada. In: G.L. Raines, R.E. Lisle, R.W. Schafer and W.H. Wilkinson (Editors), Geology and Ore Deposits of the Great Basin, Vol. II. Geol. Soc. Nev., pp. 1123–1144.

Bonham, H.F., Jr., 1989. Bulk mineable gold deposits of the western United States. In: R.R. Keays, R.H. Ramsay and D.I. Groves (Editors), The Geology of Gold Deposits: The Perspective in 1988. Econ. Geol. Monogr., 6: 193–207.

Bonham, H.F., Jr. and Hess, R.H., 1991. Bulk-mineable precious-metal deposits. In: The Nevada Mineral Industry—1990. Nev. Bur. Min. Geol., Spec. Publ., MI-1990: 19–26.

Brooks, J.W., Meinert, L.D., Kuyper, B.A. and Lane, M.L., 1991. Petrology and geochemistry of the McCoy gold skarn, Lander County, Nevada. In: G.L. Raines, R.E. Lisle, R.W. Schafer and W.H. Wilkinson (Editors), Geology and Ore Deposits of the Great Basin, Vol. II. Geol. Soc. Nev., pp. 419–442.

Byers, F.M., Jr., Carr, W.J. and Orkild, P.P., 1976. Volcanic suites and cauldrons of Timber Mountain–Oasis Valley Caldera Complex, Southern Nevada. U.S. Geol. Surv. Prof. Pap., 919, 70 pp.

Byers, F.M., Jr., Carr, W.J. and Orkild, P.P., 1989. Volcanic centers of southwestern Nevada: evolution of understanding, 1960–1988. J. Geophys. Res., 94 (B5): 5908–5924.

Capps, R.C. and Moore, J.A., 1991. Geologic setting of mid-Miocene gold deposits in the Castle Mountains, San Bernardino County, California and Clark County, Nevada. In: G.L. Raines, R.E. Lisle, R.W. Schafer and W.H. Wilkinson (Editors), Geology and Ore Deposits of the Great Basin, Vol. II. Geol. Soc. Nev., pp. 1195–1219.

Carr, M.D. and Monsen, S.A., 1988. A field trip guide to the geology of Bare Mountain. In: D.L. Wide and M.L. Faber (Editors), This Extended Land—Geological Journeys in the Southern Basin and Range. Geol. Soc. Am., Cordilleran Section, Field Trip Guidebook, pp. 50–57.

Carr, W.J., 1984. Regional structural setting of Yucca Mountain, southwestern Nevada, and late Cenozoic rates of tectonic activity in part of the southwestern Great Basin, Nevada and California. U.S. Geol. Surv., Open-File Rep., 84-854, 114 pp.

Carr, W.J., Byers, F.M. and Orkild, P.P., 1986. Stratigraphic and volcano-tectonic relations of Crater Flat Tuff and some older volcanic units, Nye County, Nevada. U.S. Geol. Surv. Prof. Pap., 1323, 23 pp.

Castor, S.B., Feldman, S.C. and Tingley, J.V., 1990. Mineral evaluation of the Yucca Mountain Addition, Nye County, Nevada. Nev. Bur. Min. Geol., Open-File Rep., 90-4, 107 pp.

Christiansen, R.L., Lipman, P.W., Carr, W.J., Byers, F.M., Jr., Orkild, P.P. and Sargent, K.A., 1977. Timber Mountain–Oasis Valley caldera complex of southern Nevada. Geol. Soc. Am. Bull., 88: 943–959.

Cornwall, H.R., 1972. Geology and mineral deposits of southern Nye County, Nevada. Nev. Bur. Min. Geol. Bull., 77, 49 pp.

Cornwall, H.R. and Kleinhampl, F.J., 1961. Geology of the Bare Mountain quadrangle. U.S. Geol. Surv. Map GQ-157, 1:62,500 scale.

Cornwall, H.R. and Kleinhampl, F.J., 1964. Geology of the Bullfrog quadrangle and ore deposits related to the Bullfrog Hills caldera, Nye County, Nevada, and Inyo County, California. U.S. Geol. Surv. Prof. Pap., 454-J, 25 pp.

Couch, B.F. and Carpenter, J.A., 1943. Nevada's metal and mineral production. Nev. Bur. Min. Geol. Bull., 38, 159 pp.

Dowling, K. and Morrison, G., 1989. Application of quartz textures to the classification of gold deposits using North Queensland examples. In: R.R. Keays, R.H. Ramsay and D.I. Groves (Editors), The Geology of Gold Deposits: The Perspective in 1988. Econ. Geol. Monogr., 6: 342–355.

Ekren, E.B. and Sargent, K.A., 1965. Geologic map of the Skull Mountain quadrangle, Nye County, Nevada. U.S. Geol. Surv. Map GQ-387, 1:24,000 scale.

Greybeck, J.D. and Wallace, A.B., 1991. Gold mineralization at Fluorspar Canyon near Beatty, Nye County, Nevada. In: G.L. Raines, R.E. Lisle, R.W. Schafer and W.H. Wilkinson (Editors), Geology and Ore Deposits of the Great basin, Vol. II. Geol. Soc. Nev., pp. 935–946.

Hamilton, W.B., 1988. Detachment faulting in the Death Valley region. California and Nevada. U.S. Geol. Surv. Bull., (1790): 51–85.

Hausback, B.P., Deino, A.L., Turrin, B.T., McKee, E.H., Frizzell, V.A., Noble, D.C. and Weiss, S.I., 1990. New $^{40}Ar/^{39}Ar$ ages for the Spearhead and Civet Cat Canyon Members of the Stonewall Flat Tuff, Nye County, Nevada: Evidence for systematic errors in standard K-Ar age determinations on sanidine. Isochron/West, 56: 3–7.

Heald, P., Foley, J.K. and Hayba, D.O., 1987. Comparative anatomy of volcanic-hosted epithermal deposits: acid-sulfate and adularia-sericite types. Econ. Geol., 82: 1–26.

Hill, R.H., Adrian, B.M., Bagby, W.C., Bailey, E.A., Goldfarb, R.J. and Pickthorn, W.J., 1986. Geochemical data for rock samples collected from selected sediment-hosted disseminated precious-metal deposits in Nevada. U.S. Geol. Surv. Open-File Rep. 86-107, 30 pp.

Hoover, D.B., Chornack, M.P., Nervick, K.H. and Broker, M.M., 1982. Electrical studies at the proposed Wahmonie and Calico Hills nuclear waste sites, Nevada Test Site, Nye County, Nevada. U.S. Geol. Surv. Open-File Rep., 82-466, 45 pp.

Jackson, M.R., Jr., 1988. The Timber Mountain magmato-thermal event: an intense widespread culmination of magmatic and hydrothermal activity at the southwestern Nevada volcanic field. Unpubl. MSc thesis, Univ. Nevada, Reno, Nev., 46 pp.

Jorgensen, D.K., Rankin, J.W. and Wilkins, J., Jr., 1989. The geology, alteration, and mineralogy of the Bullfrog gold deposit, Nye County, Nevada. Soc. Min. Eng., Preprint 89-135, 13 pp.

Kistler, R.W., 1968. Potassium-argon ages of volcanic rocks in Nye and Esmeralda Counties, Nevada. Geol. Soc. Am. Mem., 110: 251–263.

Lechler, P.L. and Desilets, M.O., 1991. The NBMG standard reference material project. Nev. Geol., 10: 1–2.

Maldonado, F., 1990a. Structural geology of the upper plate of the Bullfrog Hills detachment fault system, southern Nevada. Geol. Soc. Am. Bull., 102: 992–1006.

Maldonado, F., 1990b. Geologic map of the northwest quarter of the Bullfrog 15-minute quadrangle, Nye County, Nevada. U.S. Geol. Surv. Map I-1985, 1:24,000 scale.

Maldonado, F. and Hausback, B.P., 1990. Geologic map of the northeast quarter of the Bullfrog 15-minute quadrangle, Nye County, Nevada. U.S. Geol. Surv. Map I-2049, 1:24,000 scale.

Mapa, M.R., 1990. Geology and mineralization of the Mother Lode mine, Nye County, Nevada. In: R.H. Buffa and A.R. Coyner (Editors), Geology and Ore Deposits of the Great Basin Symposium, April 1990; Field Trip Guidebook Compendium. Geol. Soc. Nev., pp. 1076–1077.

Marvin, R.F., Mehnert, H.H. and Naeser, C.W., 1989. U.S. Geological Survey radiometric ages—compilation "C", part 3: California and Nevada. Isochron/West, 52: 3–11.

Moeller, S.A., 1988. Geology and mineralization in the Candelaria district. Mineral County, Nevada. In: R.W. Schafer, J.J. Cooper and P.G. Vikre (Editors), Bulk Mineable Precious Metal Deposits of the Western United States Symp. Proc., Geol. Soc. Nev., pp. 135–158.

Monsen, S.A., Carr, M.D., Reheis, M.C. and Orkild, P.P., 1990. Geologic map of Bare Mountain, Nye County, Nevada. U.S. Geol. Surv. Open-File Rep. 90-25, 17 pp.

Morton, J.L., Silberman, M.L., Bonham, H.F., Garside, L.J. and Noble, D.C., 1977. K-Ar ages of volcanic rocks, plutonic rocks, and ore deposits in Nevada and eastern California. Isochron/West, 20: 19–29.

Nash, J.T., Frey, D.L., Motooka, J.M. and Siems, D.F., 1990. Geochemical analyses of ore and host rocks, Sleeper gold-silver deposit, Humboldt County, Nevada. U.S. Geol. Surv. Open-File Rep., 90-702A, 69 pp.

Noble, D.C., Weiss, S.I. and Green, S.M., 1989. High-sal-

inity fluid inclusions suggest that Miocene gold deposits of the Bare Mtn. district, NV, are related to a large buried rare-metal rich magmatic system. Geol. Soc. Am., Abstr. with Progr., 20(3): 123.

Noble, D.C., Weiss, S.I. and McKee, E.H., 1991. Magmatic and hydrothermal activity, caldera geology, and regional extension in the western part of the southwestern Nevada volcanic field. In: G.L. Raines, R.E. Lisle, R.W. Schafer and W.H. Wilkinson (Editors), Geology and Ore Deposits of the Great Basin, Vol. II. Geol. Soc. Nev., pp. 913–934.

Odt, D.A., 1983. Geology and geochemistry of the Sterling gold deposit, Nye County, Nevada. Unpubl. M.Sc. thesis, Univ. Nevada, Reno—Mackay School of Mines, Reno, Nev., 100 pp.

Orkild, P.P., 1968. Geologic map of the Mine Mountain Quadrangle, Nye County, Nevada. U.S. Geol. Surv., Map GQ-746, 1:24,000 scale.

Page, B.M., 1959. Geology of the Candelaria mining district, Mineral County, Nevada. Nev. Bur. Mines Geol. Bull., 56, 67 pp.

Papke, K.G., 1979. Fluorspar in Nevada. Nev. Bur. Mines Geol. Bull., 93: 40–47.

Percival, T.J., Bagby, W.C. and Radtke, A.S., 1988. Physical and chemical features of precious metal deposits hosted by sedimentary rocks in the western United States. In: R.W. Schafer, J.J. Cooper and P.G. Vikre (Editors), Bulk Mineable Precious Metal Deposits of the Western United States. Symp. Proc., Geol. Soc. Nev., pp. 11–34.

Percival, T.J., Radtke, A.S. and Bagby, W.C., 1990. Relationships among carbonate-replacement gold deposits, gold skarns and intrusive rocks, Bau mining district, Sarawak, Malaysia. Min. Geol., 40: 1–16.

Ponce, D.A., 1981. Preliminary gravity investigations of the Wahmonie site, Nevada Test Site, Nye County, Nevada. U.S. Geol. Surv. Open-File Rep. 81-522, 64 pp.

Quade, J., Tingley, J.V., Bentz, J.L. and Smith, P.L., 1984. A mineral inventory of the Nevada Test Site and portions of Nellis Bombing and Gunnery Range, southern Nye County, Nevada. Nev. Bur. Mines Geol. Open-File Rep. 84-2, 68 pp.

Radtke, A.S., 1985. Geology of the Carlin gold deposit, Nevada. U.S. Geol. Surv., Prof. Pap., 1262, 124 pp.

Ransome, F.L., Emmons, W.H. and Garrey, G.H., 1910. Geology and ore deposits of the Bullfrog district, Nevada. U.S. Geol. Surv. Bull. 407, 129 pp.

Sander, M.V. and Einaudi, M.T., 1990. Epithermal deposition of gold during transition from propylitic to potassic alteration at Round Mountain, Nevada. Econ. Geol., 85: 285–311.

Sawyer, D.A., Fleck, R.J., Lanphere, M.A., Warren, R.G. and Broxton, D.E., 1990. Episodic volcanism in the southwestern Nevada volcanic field: new $^{40}Ar/^{39}Ar$ geochronologic results (abstract). EOS, Trans. Am. Geophys. Union, 71: 1296.

Silitoe, R.H. and Bonham, H.F., Jr., 1990. Sediment-hosted gold deposits: distal products of magmatic-hydrothermal systems. Geology, 18: 157–161.

Stewart, J.H., 1988. Tectonics of the Walker Lane belt, western Great Basin—Mesozoic and Cenozoic deformation in a zone of shear. In: W.G. Ernst (Editor), Metamorphism and Crustal Evolution of the Western United States. Rubey Vol. VII. Prentice-Hall, Englewood Cliffs, NJ., pp. 683–713.

Thompson, A.J.B., 1991. Characteristics of acid-sulfate alteration in the Marysvale—Pioche mineral belt: a guide to gold mineralization. Utah Geol. Miner. Surv. Misc. Publ., 9-12, 29 pp.

Tingley, J.V., 1984. Trace element associations in mineral deposits, Bare Mountain (fluorine) mining district, Southern Nye County, Nevada. Nev. Bur. Mines Geol. Rep. 39, 28 pp.

Tingley, J.V. and Berger, B.R., 1985. Lode gold deposits of Round Mountain, Nevada. Nev. Bur. Mines Geol. Bull., 100, 62 pp.

Weiss, S.I., Connors, K.A., Noble, D.C. and McKee, E.H., 1990. Coeval crustal extension and magmatic activity in the Bullfrog Hills during the latter phases of Timber Mountain volcanism. Geol. Soc. Am. Abstr. with Progr., 22: 92–93.

Geology and Ore Deposits of the Great Basin

Symposium Proceedings

Editors: Gary L. Raines, Richard E. Lisle
Robert W. Schafer, and William H. Wilkinson

Sponsored by the Geological Society of Nevada
and United States Geological Survey
April 1-5, 1990

Published by
Geological Society of Nevada
Reno, Nevada 1991

Concealed Mineral Deposits in Nevada – Insights from Three-Dimensional Analysis of Gravity and Magnetic Anomalies

Richard J. Blakely and Robert C. Jachens

U. S. Geological Survey, Menlo Park, CA 94025

Introduction

Pre-Tertiary basement is exposed over only about 20 percent of the area of Nevada, yet this 20 percent is host to two-thirds of the base and precious metal deposits and prospects in the state (Maureen Sherlock, oral commun., 1988). Basement rocks buried beneath Cenozoic volcanic and sedimentary deposits presumably are similarly endowed and could be targets for mineral exploration in areas where the Cenozoic cover is thin. Quantitative interpretations of gravity data can provide information on the depth to basement beneath Cenozoic rocks and thereby help identify accessible target areas.

Magnetic interpretations complement gravity interpretations by providing information on igneous rocks. Magnetic anomalies commonly occur over areas where volcanic and plutonic rocks crop out, and the pattern of magnetic anomalies is often diagnostic of rock type. Consequently, it is possible to predict from the pattern of magnetic anomalies where volcanic and plutonic rocks are located at shallow depth beneath less magnetic rocks, an important constraint for regional mineral appraisals insofar as igneous rocks are associated with mineral commodities.

Analysis of Gravity Data

Analysis of regional gravity data from Nevada was undertaken with two main objectives: to define the location and shape of the surface of pre-Tertiary basement and to produce a gravity map that reflects variations of density within the pre-Tertiary basement. Both objectives contribute directly to the analysis of mineral resources of Nevada, the first by specifying the three-dimensional distribution of potential host rocks, and the second by placing constraints on the density and, therefore, the permissible lithology of concealed basement.

The most striking characteristic of the isostatic residual gravity map of Nevada (Fig. 1) is the pervasive regional pattern of long, narrow gravity highs and lows. This anomaly pattern is closely correlated with both the local topography and near-surface geology and reflects the strong difference in density between the rocks that make up the basement and the materials that overlie them. A longer wavelength pattern of gravity variations also is apparent on the residual gravity map, most readily seen as broad regions of high gravity in the northern and southern parts of the state compared to generally lower values present throughout the center. This broader pattern is an expression of density variations within the pre-Tertiary basement.

We have developed a method which, for the most part, succeeds in separating the observed isostatic residual gravity field of Nevada into its component parts: the field caused by density variations within the basement, and the field caused by variations in thickness of young cover. The process is an iterative one. The estimate of basement gravity starts by using only gravity stations located on exposed basement. The estimate then is refined by successive attempts to remove the effects of Cenozoic cover using an empirical density-depth function.

The primary products of this separation procedure are shown in Figures 2 and 3. Figure 2 shows the gravity field produced by pre-Tertiary basement. The pervasive short-wavelength grain of the original residual anomaly (Fig. 1) has been eliminated, yet the major long-wavelength features persist. The dominant, first-order feature of the basement gravity of Nevada (Fig. 2) is the enormous area of low gravity that spans the entire state between lat 37deg and 40.5deg N. The regional gravity low reflects sources within the pre-Tertiary basement, but its strongest geologic correlation is with the distribution of middle Tertiary silicic ash-flow tuffs. The broad gravity low may reflect silicic intrusions within the middle and upper crust that are the counterparts of the volcanic rocks at the surface.

The map showing the thickness of Cenozoic cover (Fig. 3) suggests that a vast area of Nevada may have basement at relatively shallow depth. Although about 80 percent of the state is covered by Cenozoic deposits, Figure 3 shows that these deposits are thicker than 1 km only over about 20 percent of the state. Consequently, 60 percent of the state is covered by Cenozoic deposits sufficiently thin that pre-Tertiary basement rocks are within reach of current exploration techniques.

The cover-thickness map also reflects late Tertiary deformation in Nevada. Linear basins, volcanic depressions, and large areas of thick volcanic deposits are all evident on Figure 3. The distribution of these features

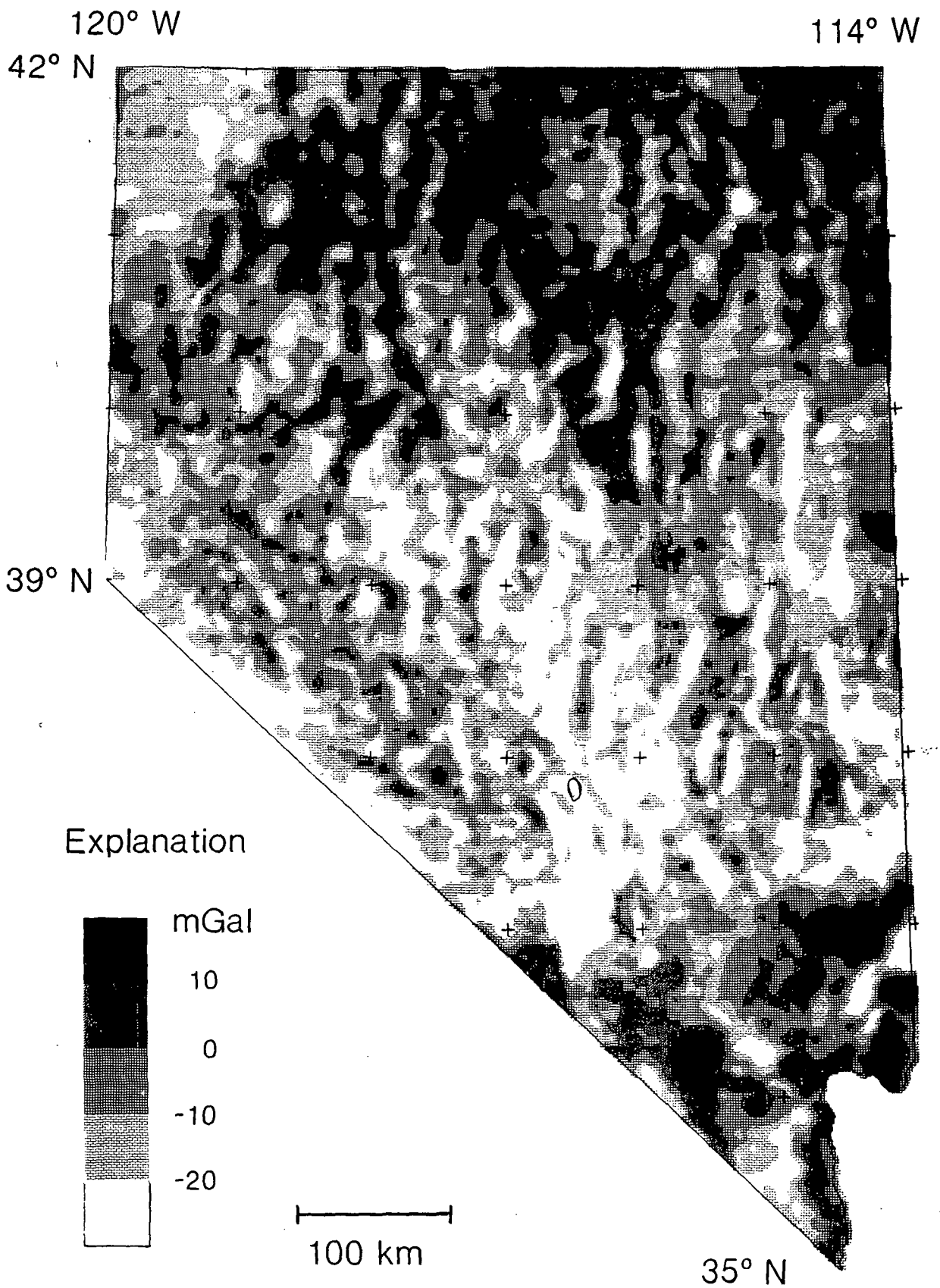

Fig. 1. Isostatic residual gravity map of Nevada. Contour interval 10 mGal. Data from Saltus (1988).

indicates that late Tertiary deformation has not been uniform over the state; distinct areas with consistent deformation patterns can be recognized. The west-central part of the state, for example, is characterized by northwest-trending, generally shallow basins. This area includes much of the Walker Lane belt of Stewart (1988). In contrast, the amagmatic zone in southern Nevada has fewer and more scattered basins than surrounding areas.

Thick sequences of Tertiary volcanic rock occur in numerous places in Nevada. Calderas of the southwestern Nevada volcanic field that contain 16-6.5 Ma volcanic deposits (Byers and others, 1989) many kilometers thick (Snyder and Carr, 1984) show prominently on Figure 3, while deposits of similar age located due east appear to be much thinner. Two large areas of northern Nevada, one in the extreme northwestern corner and the other along the northern border at long 117deg W., are blanketed by volcanic rocks having ages in the range 6-17 Ma (Stewart, 1980). Although the two areas appear quite similar on geologic maps, Figure 3 indicates that the northwestern corner contains a thick volcanic sequence whereas the deposits in the north-central area are either substantially thinner or have densities nearly equal to underlying basement. The crust in the northwestern corner of Nevada must be dramatically different from anywhere else in the state.

Analysis of Magnetic Data

Two compilations of aeromagnetic data were used in the interpretations described herein. Aeromagnetic data from Nevada (Fig. 4) compiled by Hildenbrand and Kucks (1988) from 38 separate surveys were used for insights into the regional tectonic framework of the area. A second regional survey, acquired under contract to the U.S. Department of Energy as part of the National Uranium Resource Evaluation (NURE) program, was used in our interpretations. The NURE survey includes the entire conterminous United States plus Alaska and varies widely in flight specifications. In Nevada, flightlines were spaced roughly 5 km apart, except in the Death Valley and part of the Kingman 1deg by 2deg quadrangles where flightlines were spaced approximately 1.6 km apart. NURE profiles were measured approximately 120 m above terrain, and this low altitude provides a significant advantage in the detection of shallow magnetic sources.

NURE magnetic profiles were plotted along flightlines at 1:250,000 scale. Boundaries between areas with and areas without shallow (< 1 km) magnetic sources were sketched on each map based on patterns of anomalies along individual profiles. Specific anomalies were selected in areas where source depth was ambiguous; these anomalies were analyzed with the method of Peters (1949) to provide estimates of depth to magnetic source at these discrete locations. We also applied a computer-based method to estimate depth to source, modified from Blakely and Hassanzadeh (1981), to all NURE data from Nevada in order to aid and modify the above qualitative interpretation. Boundaries were subsequently digitized and merged into the statewide compilation discussed below.

Areas of Nevada with magnetic sources interpreted to be within 1 km of the surface are shown in Figure 5. This analysis shows that 46 percent of the state of Nevada is underlain by magnetic sources within 1 km of the surface, a testimony to the widespread magmatic events that accompanied the Mesozoic and Cenozoic tectonic development of this region. Figure 5 shows the location of shallow magnetic sources only. Some anomalies in aeromagnetic compilations are caused by deep magnetic sources with no shallow counterparts and are not expected to appear in Figure 5. The so-called Charleston Peak anomaly (Fig. 4, lat 36deg00' N., long 115deg00' W.) in the amagmatic zone of southern Nevada, for example, is a significant feature of most aeromagnetic compilations. The source of this anomaly is buried several kilometers below the topographic surface (Blank, 1988) and, therefore, does not appear in our map of shallow magnetic sources.

Aeromagnetic compilations (Fig. 4) show a narrow anomaly with north-northwest trend extending 280 km through north-central Nevada. The association of this anomaly in some locations with basaltic and andesitic extrusive and intrusive rocks suggests that similar rocks exist along the entire length of the anomaly, and the feature has been interpreted as a rift zone active during the middle Miocene (for example, Zoback and Thompson, 1978). Two hot-spring gold deposits are associated with basaltic rocks of the northern Nevada rift, and other hot-spring gold deposits and several hot-spring mercury deposits are associated with similar anomalies to the west (Cox and others, this volume). Contoured aeromagnetic maps show that the northern Nevada rift continues south to about lat 39deg N., but interpretation of NURE profiles suggests that it extends considerably farther to the south-southeast. A narrow band of shallow magnetic sources (Fig. 5), approximately on strike with the northern Nevada rift, extends to at least lat 38deg N. and perhaps to the amagmatic zone (lat 37deg N.). Magnetic sources in this southern part of the rift are obscured by nonmagnetic cover less than 1 km thick in most locations. By analogy with the northern part of the rift, they may be targets for hot-spring gold and mercury deposits.

Magnetic anomalies in the Walker Lane belt of southwestern Nevada (Stewart, 1988) have arcuate, northwesterly trends generally parallel to the Walker Lane (Fig. 4). Blakely (1988) noted that the width of the northwest-trending pattern of magnetic anomalies is considerably wider than the belt described by Albers (1967) and Stewart and others (1968), extending in some places over 150 km north-northeast of the Walker Lane and into topography with north to northeast trends more typical of the Basin and Range province. The magnetic anomalies may indicate an underlying tectonic

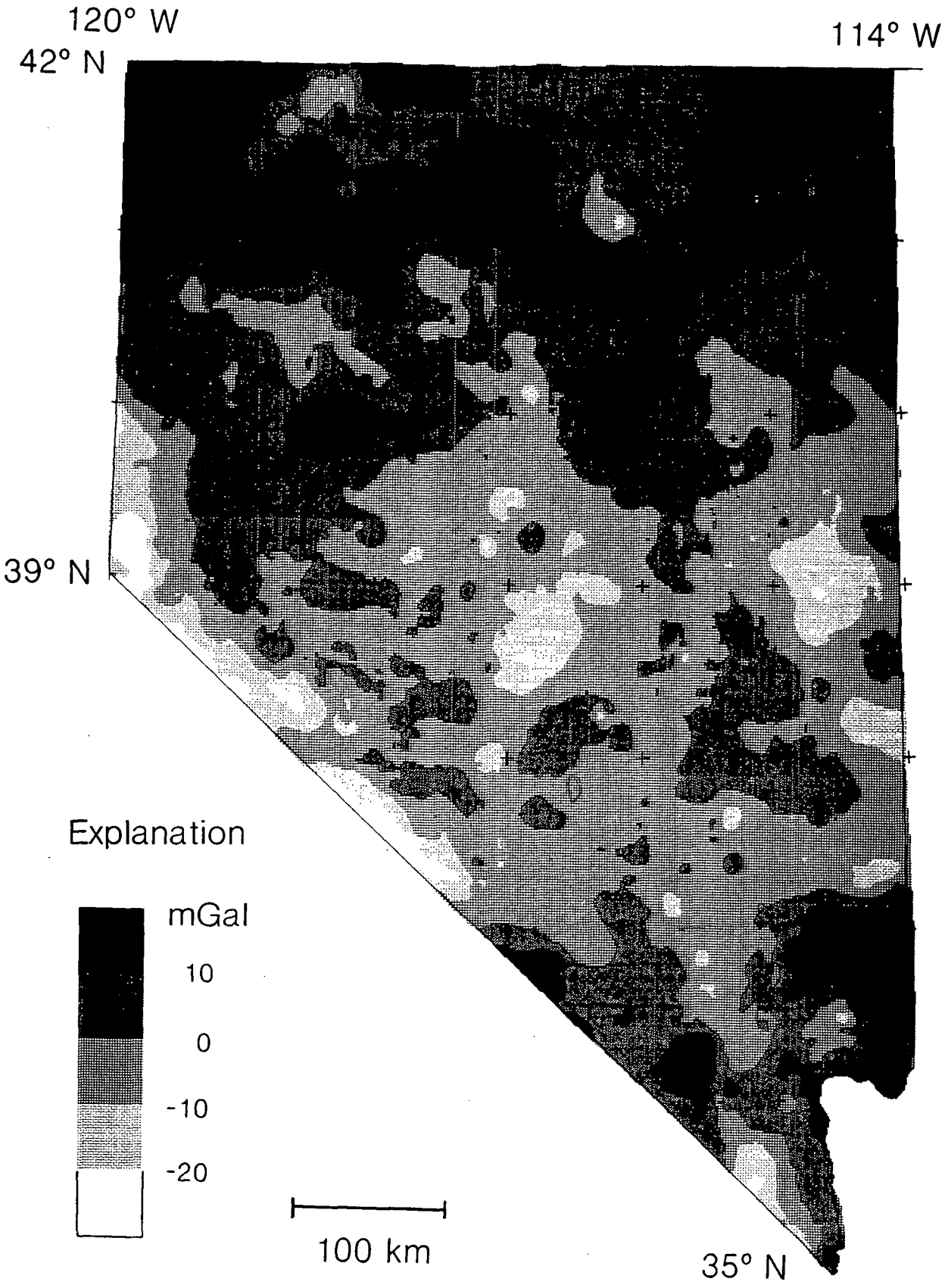

Fig. 2. Basement gravity map of Nevada. Contour interval 10 mGal.

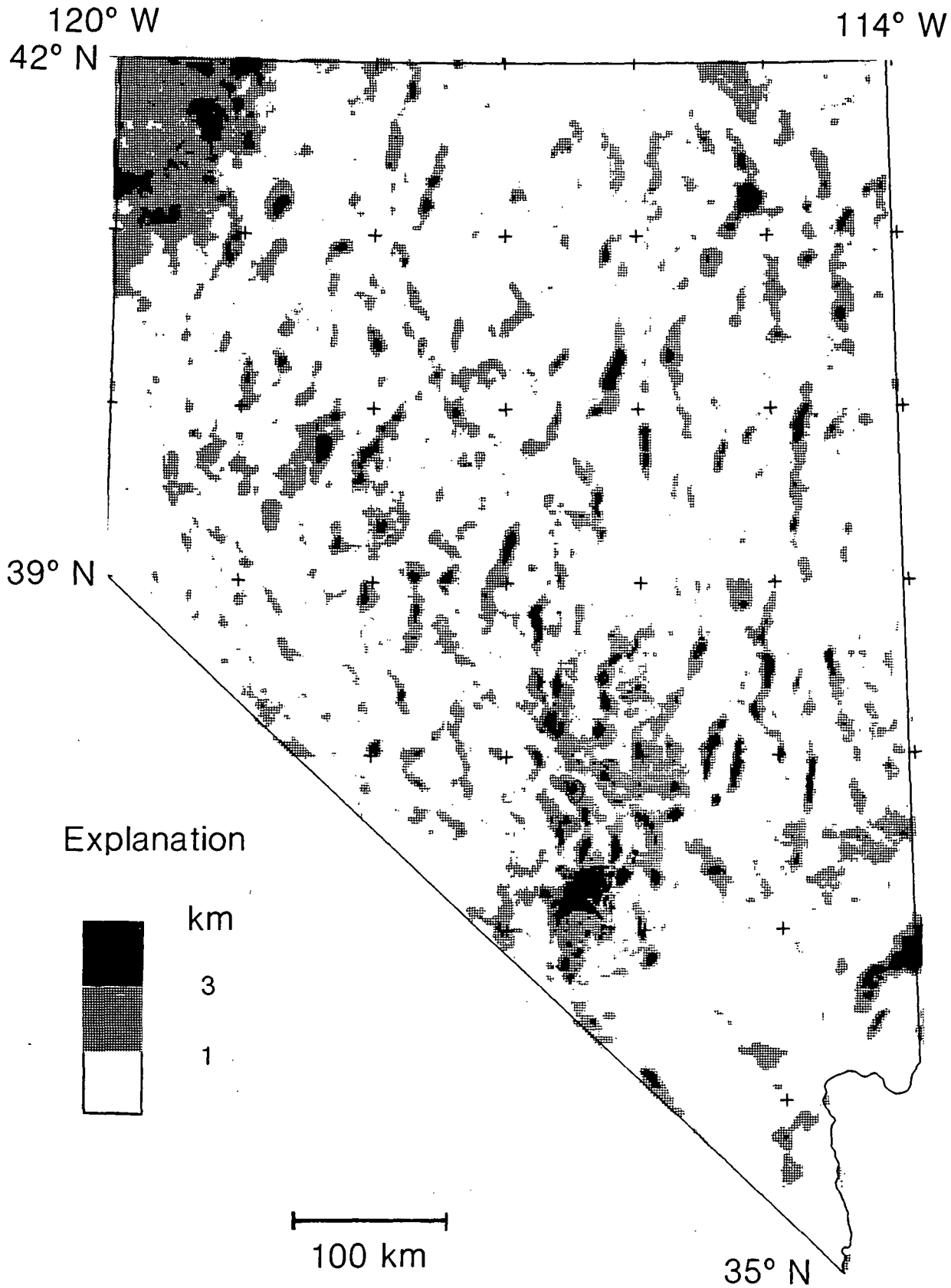

Fig. 3. Thickness of Cenozoic cover in Nevada. A constant density contrast of 0.25 g/cm3 between pre-Tertiary basement rocks and Cenozoic cover material was assumed for all regions below a depth of 1.2 km but above the basement surface.

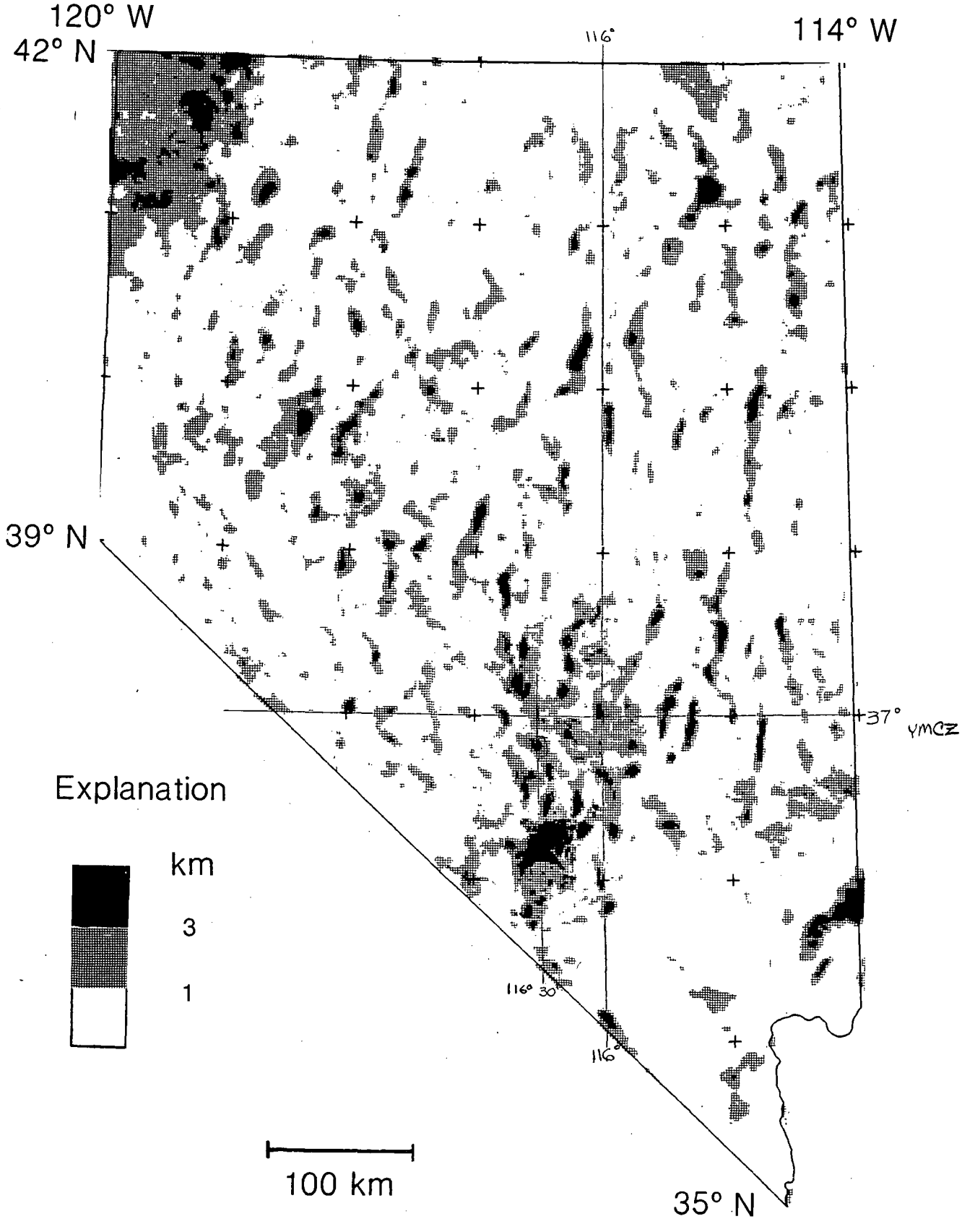

Fig. 3. Thickness of Cenozoic cover in Nevada. A constant density contrast of 0.25 g/cm3 between pre-Tertiary basement rocks and Cenozoic cover material was assumed for all regions below a depth of 1.2 km but above the basement surface.

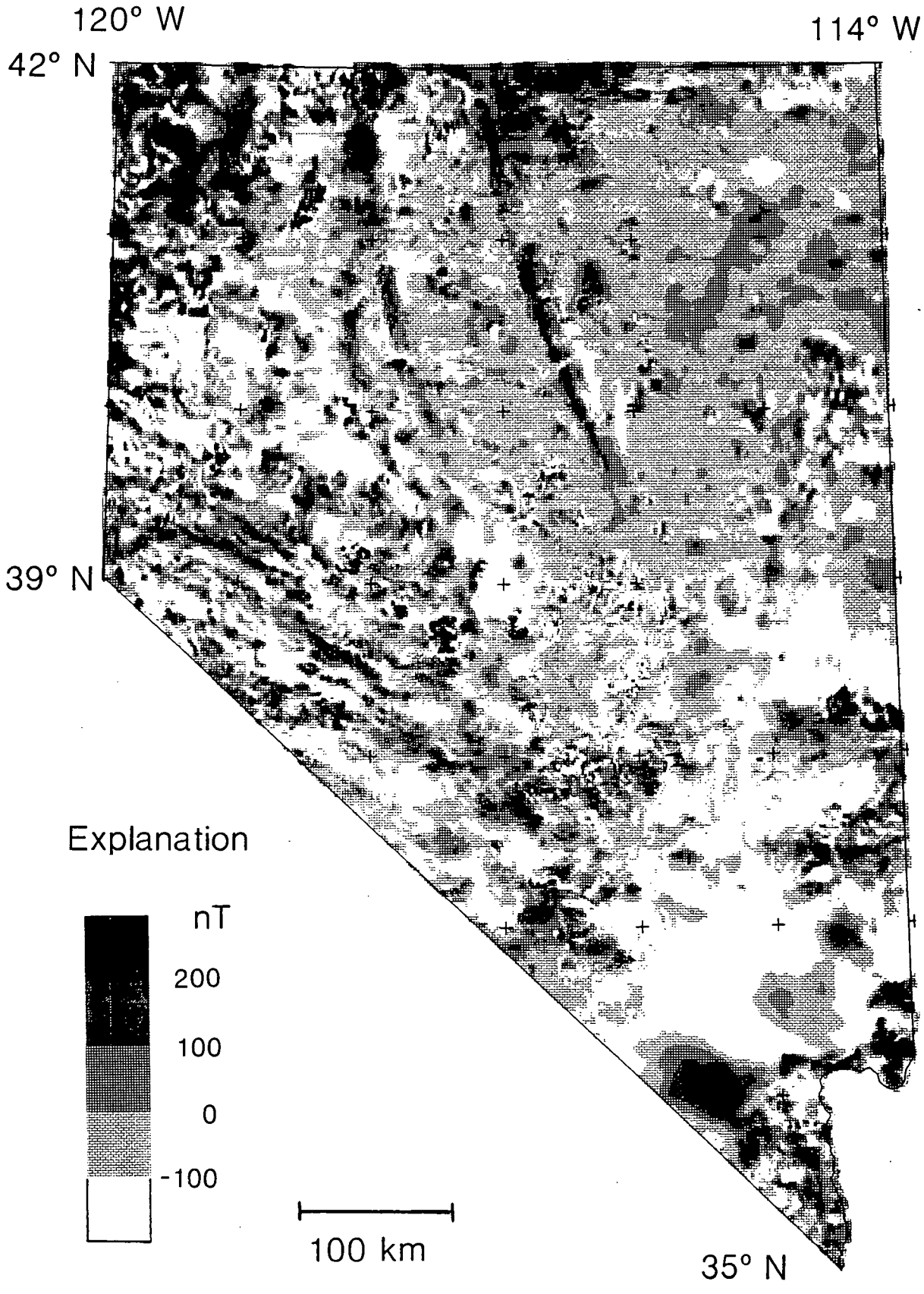

Fig. 4. Aeromagnetic anomaly map of Nevada. Total field anomalies from Nevada analytically continued to 305 m above terrain. Contour interval 100 nT. Modified from the compilation by Hildenbrand and Kucks (1988).

Fig. 5. Location of shallow magnetic sources in Nevada as interpreted from NURE magnetic profiles. Areas with magnetic sources within 1 km of the topographic surface are shown in black; areas without magnetic sources within 1 km of the surface are shown in stipple pattern. Blank area indicates insufficient data to make a reliable interpretation.

fabric older than modern topography and exposed geology. A surprising correlation between this regional magnetic anomaly pattern and the distribution of mineral deposits was noted by Cox and others (this volume). All of the volcanic-hosted epithermal deposits in southwestern Nevada are located within the Walker Lane magnetic zone. Cox and others (this volume) proposed that late-Tertiary faulting influenced the present-day magnetic anomaly patterns and was partially responsible for the distribution of volcanic-hosted deposits. Moreover, pluton-related deposits and most of the sediment-hosted gold deposits are absent from this magnetic zone, suggesting that these classes of deposits require an environment of tectonic quiescence (Cox and others, this volume).

References

Albers, J. P., 1967, Belt of sigmoidal bending and right-lateral faulting in the western Great Basin: Geological Society of America Bulletin, v. 78, p. 143-156.

Blakely, R. J., 1988, Curie temperature isotherm analysis and tectonic implications of aeromagnetic data from Nevada: Journal of Geophysical Research, v. 93, p. 11,817-11,832.

Blakely, R. J., and Hassanzadeh, Siamak, 1981, Estimation of depth to magnetic source using maximum entropy power spectra, in Crustal formation and Andean convergence: Geological Society of America Memoir 154, p. 667-682.

Blank, H. R., 1988, Basement structure in the Las Vegas region from potential-field data [abstract]: Abstracts with Programs, 84th Annual Meeting, Cordilleran Section, Geological Society of America, v. 20, p. 144.

Byers, F.M., Carr, W. J., and Orkild, Paul P., 1989, Volcanic centers of southwestern Nevada: evolution of understanding, 1960-1988: Journal of Geophysical Research, v. 94, p. 5908-5924.

Cox, D. P., Ludington, Steve, Sherlock, M. G., Singer, D. A., Berger, B. R., and Tingley, J. V., 1990, Mineralization patterns in time and space in the Great Basin of Nevada: this volume.

Hildenbrand, T. G., and Kucks, R. P., 1988, Filtered magnetic anomaly maps of Nevada: Nevada Bureau of Mines and Geology Map 93B, scale 1:1,000,000 (4 sheets) and 1:2,000,000 (1 sheet).

Peters, L. J., 1949, The direct approach to magnetic interpretation and its practical applications: Geophysics, v. 14, p. 290-320.

Saltus, R. W., 1988a, Gravity data for the state of Nevada on magnetic tape: EROS Data Center, Sioux Falls, S. Dak.

Snyder, D. B., and Carr, W. J., 1984, Interpretation of gravity data in a complex volcano-tectonic setting, southwestern Nevada: Journal of Geophysical Research, v. 89, p. 10,193-10,206.

Stewart, J. H., 1980, Geology of Nevada, a discussion to accompany the geology map of Nevada: Nevada Bureau of Mines and Geology Special Publication 4, 136 p.

Stewart, J. H., 1988, Tectonics of the Walker Lane belt, western Great Basin—Mesozoic and Cenozoic deformation in a zone of shear, in Metamorphism and crustal evolution of the western United States, Rubey volume VII, p. 683-713, Prentice Hall, Englewood Cliffs, New Jersey.

Stewart, J. H., Albers, J. P., and Poole, F. G., 1968, Summary of regional evidence for right-lateral displacement in the western Great Basin: Geological Society of America Bulletin, v. 79, p. 1407-1413.

Zoback, M. L., and Thompson, G. A., 1978, Basin and Range rifting in northern Nevada: Clues from a mid-Miocene rift and its subsequent offsets: Geology, v. 6, p. 111-116.

Alteration Mapping of the Yerington Porphyry Copper Deposit using Remote Sensing Techniques

Tod Rubin and Ronald J.P. Lyon

Department of Applied Earth Sciences, Stanford University, Stanford, CA 94305-2225

Abstract

The Yerington porphyry copper deposit is located within a Mesozoic batholith with extensive hydrothermal alteration and mineralization. Basin and Range faulting has rotated the deposit nearly 70°, so that the originally vertical hydrothermal alteration zoning is now roughly horizontal. The core of the batholith is exposed on the east flank of the Singatse Range, sericitic alteration is exposed on the west flank of the Singatse Range and in the Blue Hills to the west, and advanced argillic (alunite/pyrophyllite) alteration is exposed farther west in the Buckskin Range. The good exposures and economic value of the deposit have encouraged a remarkable amount of geologic exploration mapping and research on the system. The extensive exposures also provide an excellent opportunity for remote sensing of alteration zoning.

A large number of remote sensing devices have been used by the Stanford Remote Sensing Laboratory to study the Yerington hydrothermal system over the past 15 years. These include the spaceborne instruments Landsat MSS and Thematic Mapper, and the airborne imaging instruments NASA NS001, Daedalus 1268, NASA AIS-I and AIS-II, NASA AVIRIS, the Geophysical Environmental Research Imaging Spectrometer (GERIS), and the Geoscan Mark II Imaging Spectrometer (GeoscanII), in addition to photographic systems. The early systems such as Landsat MSS showed little more than geomorphology, iron staining, and vegetation anomalies. Thematic Mapper imagery clearly showed gross patterns of alteration. Airborne instruments, and especially the recent versions of imaging spectrometers, have sufficient spatial and spectral resolution to accurately delineate different alteration zones. In this paper we review the capabilities of the different systems for mapping alteration in a well studied and economically significant deposit.

Geology

The 10 km x 15 km zone of exploration interest runs approximately west-northwest across the Singatse and Buckskin Ranges of west central Nevada, while the ranges themselves run roughly north-south (see Fig. 1). The rock units consist mainly of lower Mesozoic sediments, Jurassic plutonic rocks and extrusive equivalents, and Tertiary ignimbritic volcanics. The Jurassic Yerington Batholith intruded the lower Mesozoic sandstones, limestones and evaporites, locally forming economic skarns. A series of hydrothermal events left a range of alteration zones in the plutonic rocks, from deeper sodic alteration through potassic and sericitic in the Singatse Range, and advanced argillic alteration in the Buckskin Range. Later faulting rotated the entire sequence nearly 70 degrees, resulting in a sub-horizontal exposure with the base of the system in the east (at the Yerington pit in the eastern the Singatse Range) and the top of the system in the west (in the Buckskin Range). This exposure presents a unique opportunity for study of porphyry systems. Parts of the system have been mapped in detail by Dilles (1983), and Proffett and Dilles (1984).

Alteration minerals absorb light at specific wavelengths as a function of their crystal chemistry (Hunt and Salisbury, 1970; Lee and Raines, 1984). The absorption features of greatest interest are those caused by FeOx (near 0.9 to 1.1 μm), the sulfate (at 1.7μm), hydroxyl (near 2.2 to 2.3 μm), and carbonate anions (at 2.3μm). Spectral signatures from several minerals are shown in Fig. 2. The distribution and abundance of minerals on the ground surface can be measured remotely if a remote sensing instrument measures the wavelengths where the minerals have absorption features. The focus of this paper will be the 2.2μm region, where hydrous alteration minerals have absorption features.

Remote Sensing Instruments

The spaceborne instruments Landsat MSS and SPOT will not be discussed in detail here because they do not measure light in the 2.2μm region. They are useful for obtaining geographic information, especially in overseas areas where basic maps are often unavailable. They are also useful for vegetation studies, but they are generally not powerful tools for alteration mapping in the Great Basin. Landsat TM data are similar to the Thematic Mapper Simulator data discussed below.

Data from the following aircraft-borne instruments will be discussed:

1. NASA NS001 (Thematic Mapper Simulator)
2. Daedalus 1268 (Thematic Mapper Simulator)

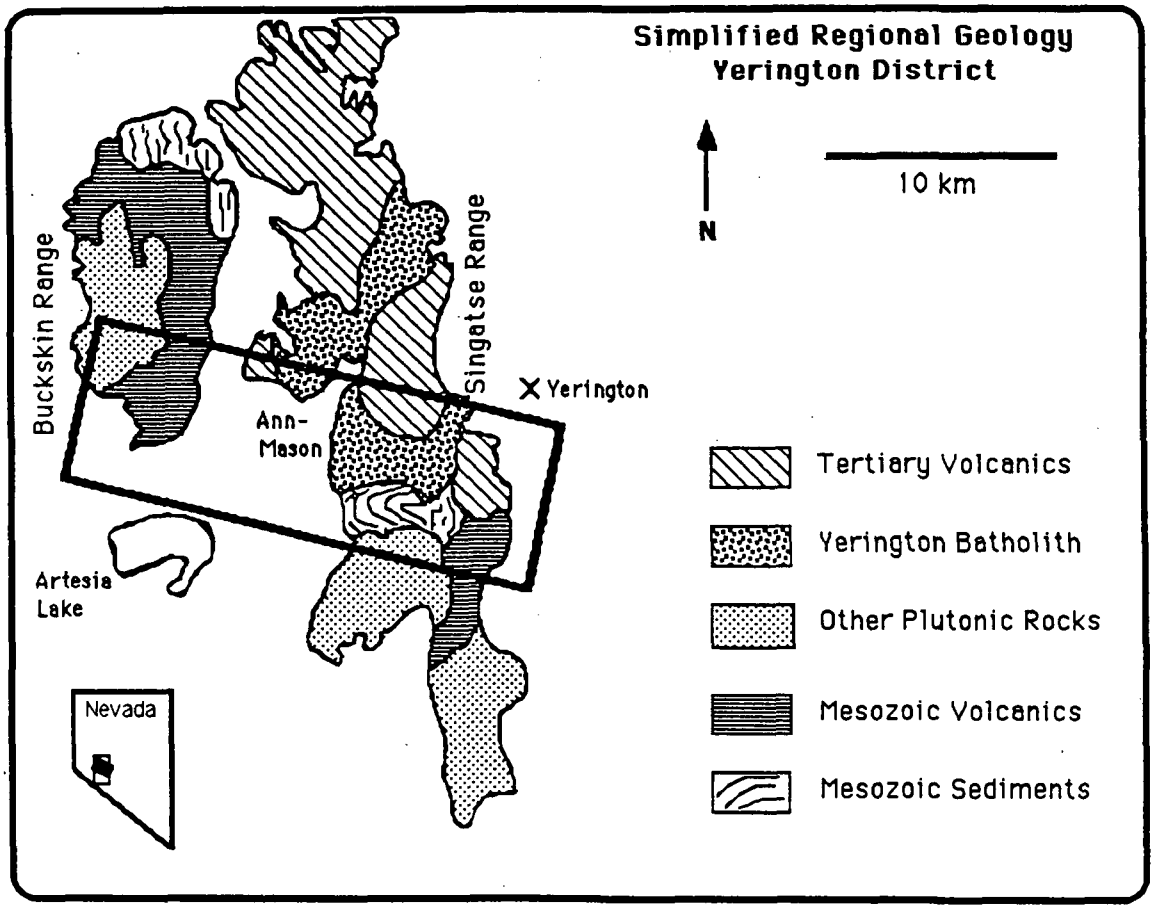

Fig. 1. Regional geologic map of the Yerington area after Dilles (1983) and Proffett and Dilles (1984). Outline shows area of exploration interest and remote sensing coverage.

3. Airborne Imaging Spectrometer (AIS-1 and AIS-2)
4. Advanced Visible and Infrared Imaging Spectrometer (AVIRIS)
5. Geophysical Environmental Research Imaging Spectrometer (GERIS)
6. Geoscan Mark II Imaging Spectrometer (Geoscan II)

The swath width and spatial and spectral resolution are different for each scanner system. Fig. 3 shows the spectral bandpasses of the most commonly used instruments. The thematic mapper simulator (TMS) systems have very good coverage of the geographic area and relatively high signal-to-noise ratios. AIS was a great improvement in spectral resolution at the expense of geographic coverage. AVIRIS further improved the spectral resolution of AIS, and with ground coverage comparable to that of the TMS systems. Early AVIRIS data had very poor signal-to-noise properties. The GERIS and Geoscan units currently have both good spectral resolution and wide geographic coverage. The images produced by the instruments are discussed below.

NASA NS001 Scanner

Number of Channels	8
Ground Resolution:	20 meters
Swath Width	14 km

Channels for display can be chosen to emphasize differentiation of rock units, and to distinguish hydrothermally altered from unaltered rock (Lyon and Lanz, 1985; Roberts et al, 1986). Different lithologic units can be recognized, and the good spatial resolution permits relatively accurate location of field sites. Easily distinguishable rock units include Tertiary felsic volcanics, the unaltered areas of the Yerington Batholith, Mesozoic clastic sediments, and gypsiferous evaporites. It is also possible to distinguish hydrothermally altered from unaltered areas within the Yerington batholith. It is not possible to reliably separate different alteration units due to the insufficient number of channels in the 2.2μm region.

Daedalus 1268 Scanner

Number of Channels	11
Ground Resolution	28 meters
Swath Width	16.6 km

Numerous different units are distinguishable, with good spatial resolution. The northwest trend of the hydrothermal system is somewhat obscured in some of the Yerington imagery by the high contrast effects due

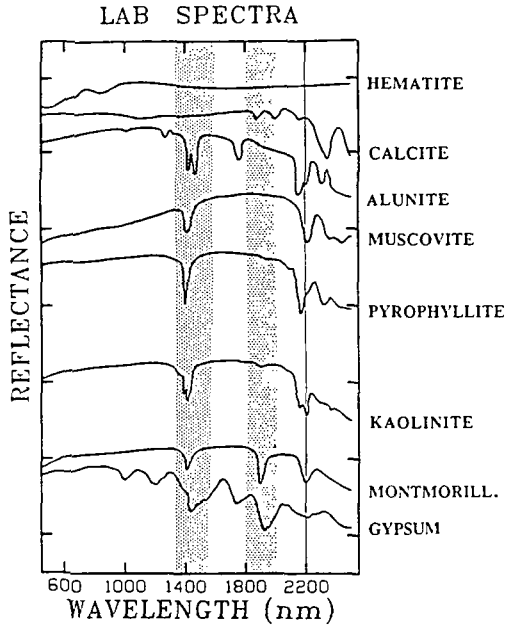

Fig. 2. Visible (0.4 - 0.7 um) and shortwave infrared spectral signatures of some minerals found at Yerington (after Lee and Raines, 1984). Stippled areas indicate wavelengths not useful for remote sensing due to atmospheric absorption.

to local topography. Detailed examination reveals the Tertiary Volcanics, the Yerington Batholith, Mesozoic clastic sediments and gypsiferous evaporites, and the Shamrock Batholith. Hydrothermally altered areas within the Yerington Batholith are clearly distinguishable from unaltered areas. Fine separation of different alteration units is not possible due to the insufficient number of channels in the 2.2μm region.

NASA AIS-2

Airborne Imaging Spectrometer	
Number of Channels	128
Ground Resolution	12 meters
Swath Width	787 m

High spectral resolution permits differentiation of both rock and alteration units (Lyon, 1986). A typical image covers a strip of ground 787 meters wide and several kilometers long. AIS imagery is of limited use due to this narrow spatial coverage. While a long strip of imagery can display a number of rock and alteration units, the geographic location of the sites is often quite difficult to establish. The data require a significant amount of preprocessing to remove the effects of the atmosphere and topography (Green and Craig, 1984).

NASA AVIRIS

Airborne Visible Infrared Imaging Spectrometer	
Number of Channels	220
Ground Resolution	20 meters
Swath Width	11 km

AVIRIS has the highest nominal spectral resolution of all the instruments discussed here, while also having wide spatial coverage. The narrow spectral bands result in a low signal-to-noise ratio, making spectral differentiation of rock and alteration units difficult (Rubin and Lyon, 1988). While the wavelengths should provide excellent discrimination of different alteration zones, the early vintage data available for this study (acquired in July 1987) were so noisy as to be of very limited value. Spatial resolution is good, allowing accurate geographic location of field sites in many of the individual channels.

GERIS

Geophysical Environmental Research Imaging Spectrometer	
Number of Channels	63
Ground Resolution	20 meters
Swath Width	11 km

The Geophysical Environmental Research Imaging Spectrometer (GERIS) measures 63 channels at wavelengths between 0.5 to 2.5μm. The bandwidth is narrow in the near-infrared spectral region and in the 2.2μm part of the shortwave infrared spectral region. The signal-to-noise ratio of early vintage data was low, requiring 2x2 pixel averaging (thus decreasing spatial resolution to 40 meters) in order to obtain useful spectral signatures. However, automated spectral recognition of different alteration types was possible (Rubin, 1989a). Newer data appear to have a much better signal-to-noise ratio. Log-residual preprocessing is required to remove the effects of the atmosphere and topography. Combined with the wide areal coverage of the system and the relatively good spatial resolution, GERIS imagery provided the first true alteration maps of Yerington based on remote sensing data (Rubin, 1989b).

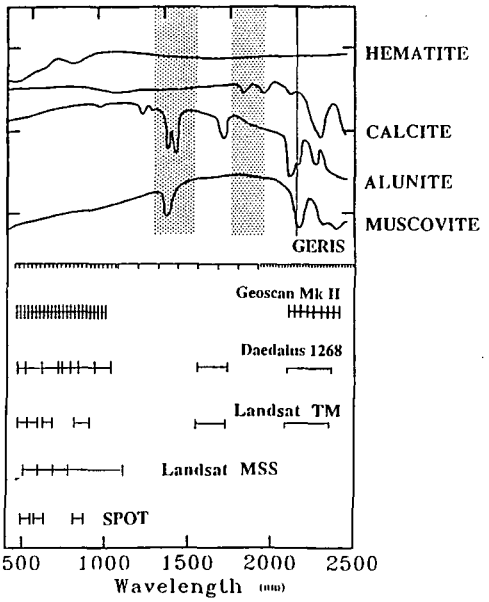

Fig. 3. Wavelength bands sampled by various remote sensing instruments. Stippled areas indicate wavelengths not useful for remote sensing due to atmospheric absorption.

Geoscan Mk II

Number of Channels	24
Ground Resolution	6 meters
Swath Width (92°)	6 km

(as flown at Yerington in July 1989)

The Geoscan Mark II represents a significant advance in both high spatial resolution and excellent signal-to-noise ratio. Narrow bands are located in the visible, the 2.2 μm, and the thermal infrared spectral regions. With 6-meter resolution data from Yerington, the imagery has the appearance of aerial photographs, making it possible to identify individual outcrops. The spectral data allow differentiation of many rock and alteration types. No preprocessing is necessary to locate areas of anomalous spectral patterns. Processing techniques have been developed to automatically recognize which particular alteration minerals (e.g. sericite, alunite, etc.) are located in the anomalous areas (Rubin, 1989a). The data reveal alteration patterns not previously recognized or mapped.

Summary

The use of many different remote sensing instruments at one well-mapped deposit has provided a unique opportunity to evaluate the different systems. Older space-borne systems such as Landsat MSS are of very little use for geologic mapping in the Great Basin, while new airborne systems have successfully reproduced both lithologic and alteration maps of great detail at Yerington. These systems have a combination of features (wide spectral range, high spectral resolution, good spatial resolution, and high signal-to-noise ratio) that provide the capability to rapidly and accurately locate altered areas, and to automatically recognize different suites of alteration minerals within those areas.

References

Dilles, J.H., 1983, The Petrology and Geochemistry of the Yerington Batholith and the Ann-Mason Porphyry Copper Deposit, Western Nevada, unpublished Stanford University PhD Thesis, 389p

Green, A.A. and Craig, M.D., 1985, Analysis of Aircraft Spectrometer Data with Logarithmic Residuals, in Airborne Imaging Spectrometer Data Analysis Workshop, 1st Pasadena, 1985, Proc: Jet Propulsion Laboratory Publication 85-41, pp111-119

Hunt, G.R., and Salisbury, J.W., 1970, Visible and Near-Infrared Spectra of Minerals and Rocks: I. Silicate Minerals: Modern Geology, v1, pp283-300

Lee, K., and Raines, G., 1984, Reflectance Spectra of Alteration Minerals, U.S. Geological Survey Open File Report # 84-096

Lyon R.J.P., and Lanz, K., 1985, Field Utilization and Analysis of 128-Channel Imagery Using Microcomputers: Applications to Yerington Nevada Field Area, *in* Airborne Imaging Spectrometer Data Analysis Workshop, 1st Pasadena, 1985, Proc: Jet Propulsion Laboratory Publication 85-41, pp35-40

Lyon, R.J.P., 1986, Comparison of the 1984 and 1985 AIS Data over the Singatse Range (Yerington) Nevada, *in* Airborne Imaging Spectrometer Data Analysis Workshop, 2nd Pasadena, 1986, Proc: Jet Propulsion Laboratory Publication 86-35, pp86-95

Proffett, J.M., and Dilles, J.H., 1984, Geologic Map of the Yerington District, Nevada,, Nevada Bureau of Mines and Geology, Map 77

Roberts, D.A., Yamaguchi, Y., and Lyon, R.J.P., 1986, Comparison of Various Techniques for Calibration of AIS Data, *in* Airborne Imaging Spectrometer Data Analysis Workshop, 2nd Pasadena, 1986, Proc: Jet Propulsion Laboratory Publication 86-35, pp21-30

Rubin, T., and Lyon, R.J.P., 1988, Comparison of Four Airborne Scanner Systems over the Ann-Mason Porphyry Copper Hydrothermal System, Yerington Nevada, *in* Thematic Conference on Remote Sensing for Exploration Geology, 6th Houston, Proc: Ann Arbor, Environmental Research Inst of Michigan, p237

Rubin, T., 1989a, Automated Spectral Recognition of Alteration Mineralogy in Imaging Spectrometer Datasets Using a Knowledge-Based Expert System. *in* International Geophysical and Remote Sensing Symposium, Vancouver, Canada, Proc: IGARSS '89, pp2065-2068

Rubin, T., 1989b, Correlation of Imaging Spectrometer and Ground Data for Alteration Mapping at Yerington, Nevada, in Thematic Conference on Remote Sensing for Exploration Geology, 7th Calgary, Proc: Ann Arbor, Environmental Research Inst of Michigan, p315-322